Received: 7 July 2022 | Revised: 5 October 2023 | Accepted: 23 October 2023

DOI: 10.1002/dep2.260

The Depositional Record Open Access
A journal of the International Association of Sedimentologists
WILEY

ORIGINAL RESEARCH ARTICLE

Sequence stratigraphical and palaeoenvironmental implications of Cenomanian–Santonian dinocyst assemblages from the Trans-Sahara epicontinental seaway: a multivariate statistical approach

Musa B. Usman[1,2] | **David W. Jolley**[1] | **Alexander T. Brasier**[1] | **Adrian J. Boyce**[3]

[1]Department of Geology and Geophysics, School of Geosciences, University of Aberdeen, Aberdeen, UK

[2]Department of Geology, Faculty of Science, Gombe State University, Gombe, Nigeria

[3]Scottish Universities Environmental Research Centre, East Kilbride, UK

Correspondence
Musa B. Usman, Department of Geology and Geophysics, School of Geosciences, University of Aberdeen, Aberdeen AB24 3UE, UK.
Email: musausman51@gmail.com

Funding information
Petroleum Technology Development Fund (PTDF) Nigeria

Abstract

The Cretaceous was punctuated by episodic flooding of continental margins forming epicontinental seas. The Trans-Sahara Seaway was one of these epicontinental seas, connecting the Gulf of Guinea with the Tethys Ocean. In this study, data including microplankton abundances, stable carbon isotopes of organic material and elemental geochemistry were integrated with traditional sedimentological analyses from the Trans-Sahara Seaway. The carbon isotopic data provide the first evidence that oceanic anoxic event 2 was present in the Trans-Sahara Seaway, and palynology shows it was associated with an increase in peridinioid dinocyst abundance. A combined study of microplankton assemblages and sedimentology reveals palaeoenvironmental trends linked to sea-level change. Lowstand system tracts were characterised by increased siliciclastic grain size, low microplankton diversity, and were dominated by Chlorophyceae. Transgressive system tracts were associated with diversity increases during rising sea level, with open marine gonyaulacoid dinocysts dominating the assemblages. Maximum flooding surfaces were recognised by the highest increase in biological diversity in argillaceous deposits. As sea level started to fall, the peridinioid dinocysts became dominant, with decreased microplankton diversity during highstand systems tracts. This combination of sedimentology and interpretation of dinocyst assemblages allows the identification of shallow to deeper marine depositional sequences of Cenomanian–Santonian strata within the Yola Sub-basin. This approach could be used to delineate marine depositional sequences where using conventional sedimentological methods alone is very challenging.

KEYWORDS

Benue Trough, dinocysts, Late Cretaceous, oceanic anoxic event 2, palaeoecology

1 | INTRODUCTION

The Cretaceous Period represented a time of high eustatic sea level (Haq et al., 1988). Late Cretaceous sea levels are estimated to have been between 100 and 250 m above those of the present day (Haq et al., 1987, 1988; Haq, 2014). Flooding of continental margins led to the formation of epicontinental seas (Allison & Wells, 2006), the rock records of which preserve evidence for oceanic anoxic events (OAEs). These purportedly global anoxic events have been put forward as the cause of widespread deposition of dark grey and black shales (Schlanger & Jenkyns, 1976). It has been proposed that heterogeneity in the degree of oxygenation recorded during OAEs could be explained by mixing of Boreal cool and Tethyan warm waters in restricted basins at peak marine transgression (Lowery et al., 2018). This suggestion was based on Late Cretaceous dinocyst distributions from epicontinental sea basins in North America, South America and Spain (Harris & Tocher, 2003; Peyrot et al., 2012; Lowery et al., 2018). Here the focus is on one of these epeiric basins, the Trans Sahara Seaway, which was located at the palaeo-equator (Figure 1), determining the microplankton palaeoecology, and applying that understanding to assist in delineating depositional sequences. The sedimentary fill deposited over the relevant time interval in this basin was largely composed of alternating dark grey and grey shale (Carter et al., 1963; Zaborski et al., 1997) with considerable potential for preserving organic microfossils.

1.1 | Dinocysts and palaeoenvironmental reconstruction

Motile dinoflagellate distribution in the water mass is controlled by light penetration, oxygenation, surface water temperature, nutrient availability, hydrodynamics and stratification of the basin (Wall et al., 1977; Powell et al., 1992; Dale, 1996). An understanding of dinoflagellate biology has previously been used to underpin palaeoecological and sequence stratigraphical interpretations of dinocyst data, particularly in combination with

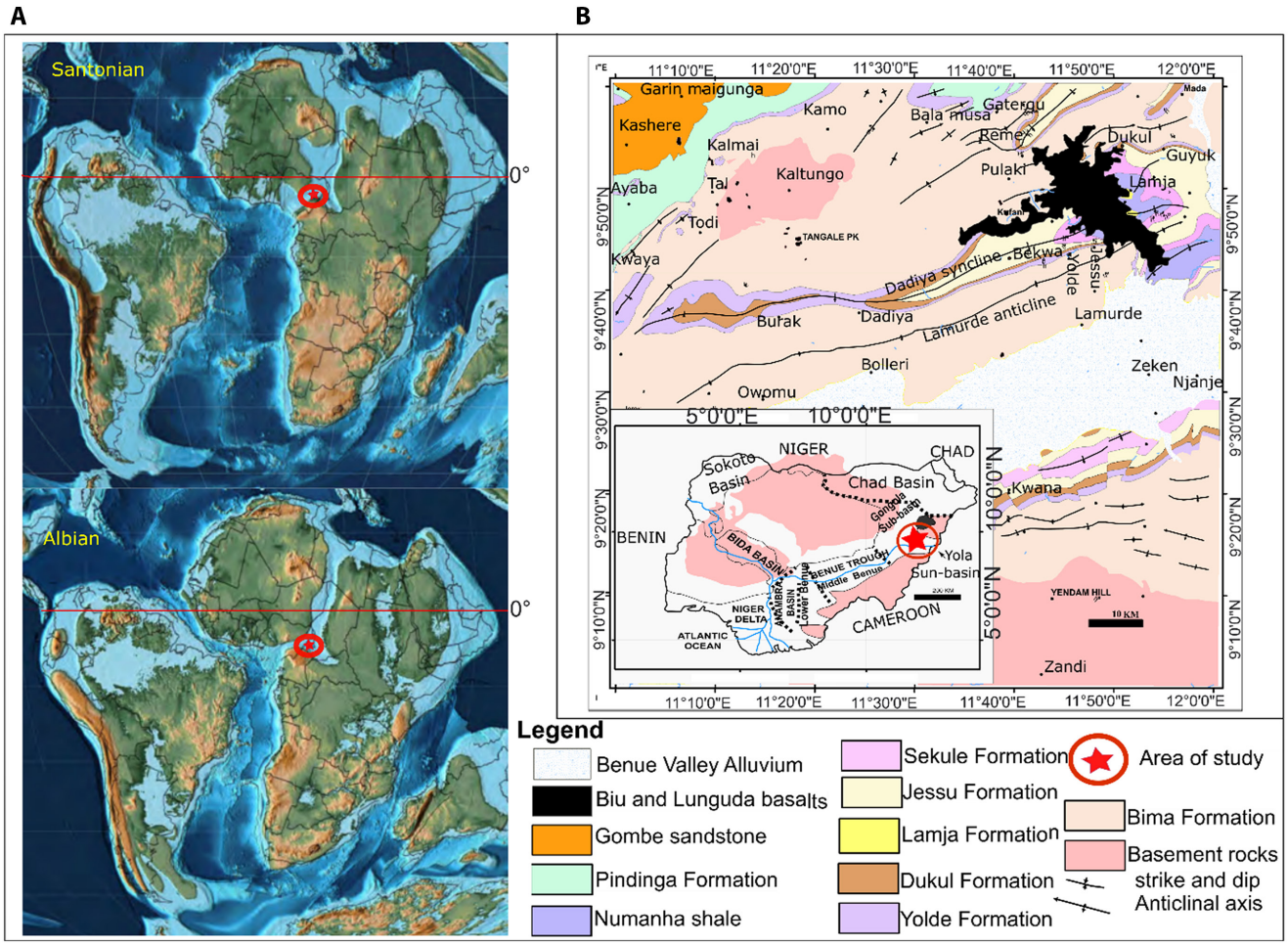

FIGURE 1 Palaeogeographic map of the study area. (A) Palaeogeographic map of the late Cretaceous showing the location of the study area (modified after Scotese, 2014). (B) Geological map showing the outcrops of Cretaceous rocks (modified after Carter et al., 1963).

stacking patterns of rock successions (Brinkhuis, 1994; Li & Habib, 1996; Powell et al., 1996; Garzon et al., 2012). In practice, the palaeoecological interpretations have mostly been based on morphometric features of dinocysts, such as process length (Li & Habib, 1996). As an example, Li and Habib (1996) interpreted longer process lengths of chorate dinocysts (e.g. *Oligosphaeridium*) as indicative of deep marine environments, and shorter process lengths of proximate to proximochorate dinocysts (e.g. *Circulodinium* and *Cyclonephelium*) as indicative of shallow marine environments. However, the reliability of using dinocyst functional morphologies for environmental interpretations can be questioned. For example, Harris and Tocher (2003) used agglomerative hierarchical cluster analysis and ratios of peridinioid and gonyaulacoid dinocyst (P/G) methods to demonstrate that some Cretaceous dinocysts previously regarded as indicators of shallow marine environments (e.g. *Circulodinium distinctum* and *Cyclonephelium membraniphorum*), were instead associated with outer shelf marine environments.

Given these results a different approach is tested rather than simply taking dinocyst morphology as a proxy for palaeoenvironment. Instead, multivariate analyses are employed to assess the palaeoenvironmental variables that plausibly controlled shifts in the microplankton assemblages during the Cenomanian–Santonian. This multivariate statistical method was chosen because it can provide a robust delineation of dinocyst palaeoecology, and because examining multiple variables together can aid in interpreting the marine depositional sequences. In the analysis presented here, ordination techniques were applied to microplankton data (including dinocysts, foraminifera test linings and Chlorophaceae) from the Yolde, Dukul, Jessu, Sekule, Numanha and Lamja formations of the Upper Benue Trough, Nigeria (described further below). These sediments were deposited in estuarine to fully marine palaeoenvironments. Many of the shifts seen in the microplankton data appear to be linked to changes observed in the depositional sequences.

2 | PALAEOGEOGRAPHY AND GEOLOGICAL SETTING

The Benue Trough formed during the opening of the Atlantic Ocean in the early Cretaceous (Genik, 1993). The Aptian–Cenomanian interval was characterised by rift events, with an influx of marine water into the Lower Benue Trough starting during the Albian (Benkhelil, 1988; Genik, 1993). In the Cenomanian–Santonian interval, the Middle and Upper Benue Trough was flooded, with the resultant narrow seaway linking up the Gulf of Guinea with the Tethys Sea (Zaborski, 2000; Benkhelil et al., 1988; Scotese, 2014; Usman et al., 2021).

The upper Benue Trough, which comprises the Gongola and Yola Sub-basins, is filled by deposits of sandstone, claystone, shale and limestone, representing continental to neritic environments. Within the Yola Sub-basin, the Cretaceous succession is composed of the Bima, Yolde, Jessu, Sekule, Numanha, and Lamja formations (Figure 2). The oldest, continental fluvial deposits of the Bima Formation unconformably overly basement rocks (Carter et al., 1963; Guiraud, 1990). The succeeding sandstone and claystones of the Yolde Formation were deposited in shallow marine shoreface environments (Sarki Yandoka et al., 2015). The Dukul Formation is composed of intercalations of limestone and claystones. Organic geochemistry of the Dukul Formation has previously been interpreted as consistent with a marine shelf depositional setting (Ayuba et al., 2020) whereas microfacies analysis was reported to be consistent with a shallow marine mid to inner ramp environment (Sarki Yandoka, 2021). The Dukul Formation is succeeded by the Jessu Formation, the latter being characterised by interbedded mudstones and light to dark grey shales, with a few beds of marl. Lithofacies analysis of the Jessu Formation carried out by Sarki Yandoka et al. (2019) showed that the formation was a progradational shoreface to offshore deposit. Overlying the Jessu Formation is the Sekule Formation which is composed of fossiliferous limestone interbedded with dark grey to grey shale. The Sekule Formation was previously interpreted simply as shallow marine (Carter et al., 1963; Usman et al., 2021). Above the Sekule Formation, the Numanha Formation is characterised by predominantly grey to brown shales and thin beds of nodular mudstones. The Numanha Formation was similarly interpreted as a shallow marine deposit by Opeloye (2012). The Yola Sub-basin is capped by the Lamja Formation that is composed of very fine to fine-grained upward-coarsening sandstone, shale, limestone and coal, interpreted as transitional marine deposits (Carter et al., 1963).

3 | METHODOLOGY

Exposures of the Bima, Yolde, Dukul, Jessu, Sekule, Numanha and Lamja formations were examined in the Upper Benue Trough. Fourteen field sections were examined, and detailed sedimentological data including colour, bedding contact, sedimentary structures, grain size, sorting and palaeocurrent directions were recorded on sedimentary logs. A total of 136 samples were collected from the outcrops with some additional samples taken from a shallow

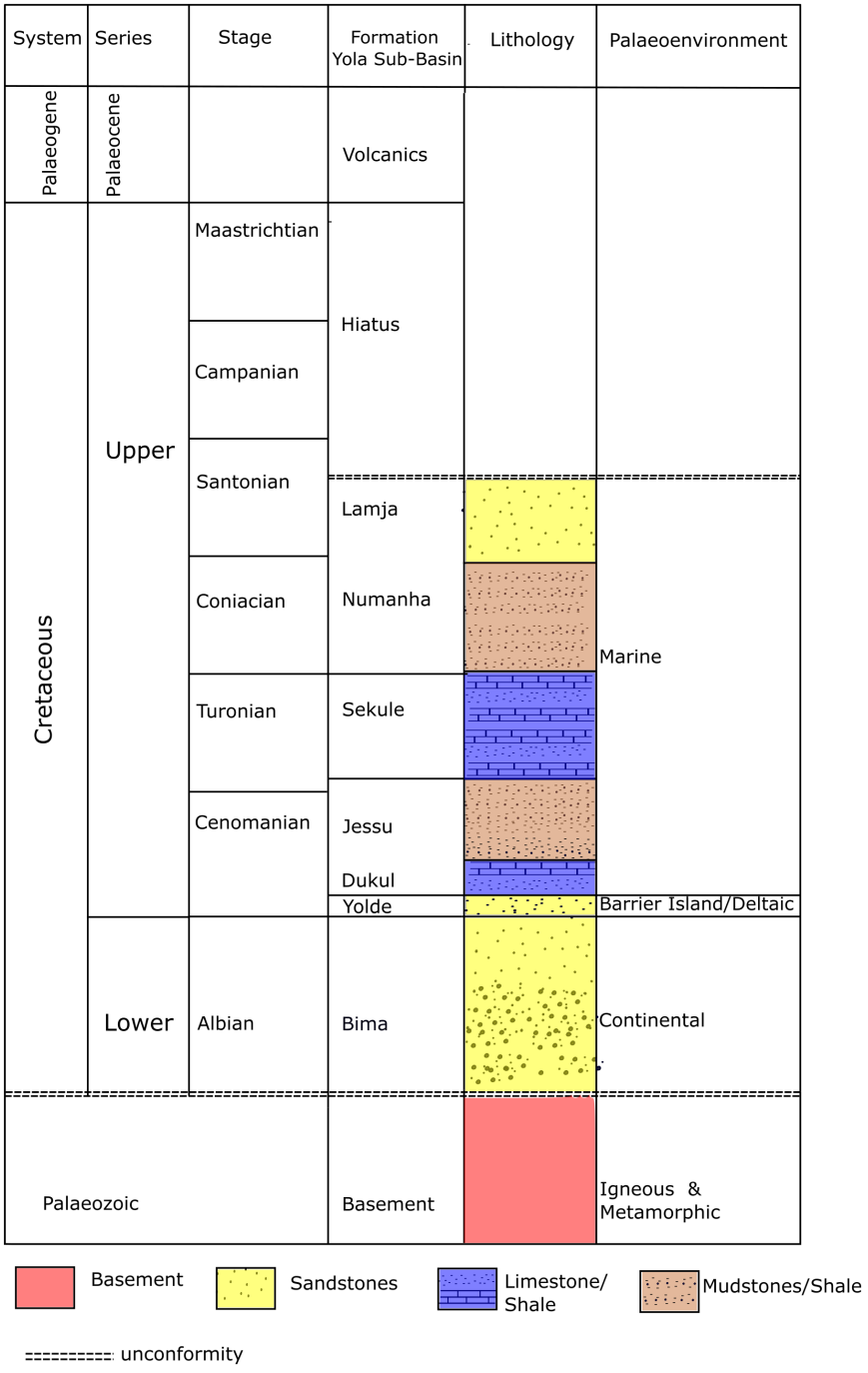

FIGURE 2 Stratigraphic chart of the Yola Sub-basin (after Usman et al., 2021).

borehole (Yolde-1). Eighty of these samples were taken from the Cenomanian–Turonian strata, which comprise the Yolde, Dukul, Jessu and Sekule formations. The remaining 56 samples were taken from the Coniacian–Santonian Numanha and Lamja formations. Microfacies analyses of the carbonate samples were conducted using a Nikon SMZ 25 Zoom Stereomicroscope, and a Nikon Microphot FX Compound microscope, both equipped with a Nikon DS Fi2 camera and Elements D software.

All samples were prepared for palynological analyses using the standard sample preparation method of Stukins et al. (2013). Hydrofluoric (HF) and hydrochloric (HCl) acids were used to remove silicate and carbonate minerals, with silicates dissolved in 40% HF for three days and decanted until neutral. The residue was then boiled in 60% HCl for 20 minutes to remove the calcium fluoride (CaF_2) precipitates, and the HCl decanted until the residues became neutral. Each of the residues were divided into two, and 70% nitric acid (NHO_3) was added for 2 to 3 minutes to one portion for some samples to oxidise the pyrite and organic matter. Slides were prepared as strew mounts from the oxidised and un-oxidised residue. These slides were

studied under an Olympus biological transmitted light microscope (Model BX53), mounted with an Olympus camera (Model SC50) at 60x magnification, in which 250 palynomorphs were counted where possible.

A calibrated portable X-ray Fluorescence (pXRF) machine (Olympus Delta Premium DP-6000 in Geochem mode) was used to determine chemical compositions. This instrument measures percent element abundances for atomic masses in the range from 24 to 238 g/mol. The samples were analysed using methods described by Saker-Clark et al. (2019); samples being crushed to a powder and placed in 20 mL vials. The samples were analysed using the pXRF and the results consist of major elements in percentage and minor elements in parts per million (ppm). Bulk analysis of the stable carbon isotope composition of organic material (carbon) was carried out on the shale samples. Samples were first powdered and then washed in a 10% HCl solution to remove carbonate contamination. Cleaned samples were analysed automatically for C isotopes on an Elementar Isoprime visION mass spectrometer set up with an on-line Pyrocube Elemental Analyser. The data are presented relative to the Vienna Pee Dee Belemnite (VPDB) standard. Internal standards run together with these samples gave reproducibility better than ±0.1‰, and the international standard USGS40 giving a value of −26.4‰ (its reported value).

3.1 | Ecological indices

Measures of assemblage diversity have been used to quantify diversity, richness and evenness in the literature (see Hammer et al., 2016). Diversity is generally controlled by stress in ecosystems, with low diversity in highly stressed ecosystems and high diversity in less stressed ecosystems (Patten, 1962; Pielou, 1969; Wall et al., 1977; Buzas, 1979; Watkins, 1989). Here, a diversity index was required that could help reveal potential sea-level driven environmental changes that could have affected dinocyst diversity. A diversity index, Shannon diversity, was used to analyse the microplankton assemblages because it uses species richness and abundance to measure assemblage disruption. As a result, it can be used to identify trends and correlations between environmental changes driven by sea-level fluctuations and microplankton diversity. An issue with the Shannon index is that it can underweight the dominant taxa and over-represent the rare taxa. To resolve this, species dominance index developed by Simpson (1949) was calculated using Palaeontological Statistic 4 (Past) software. This index is defined as:

Simpson index of dominance: $\lambda = \sum(p_i{}^2)$ where $pi = n_i/n$ (the proportion of species$_i$).

3.2 | Multivariate statistical analytical methods

Palynological data sets (the raw data being palynomorph counts) include taxa derived from different taphonomic and ecological communities. To understand these depositional environments, the palynological data set was analysed using a statistical ordination method, detrended correspondence analysis (DCA). The most commonly applied multivariate statistical method is principal component analysis (PCA). However, the PCA method assumes a linear response, which is unsuitable for this data set. Detrended correspondence analysis is preferred here for ecological data analysis, in part as it has the advantage that it is free from a linear response assumption (Hill & Gauch, 1980; Hammer et al., 2016). Developed to correct the arch effect and squeezing of the ordination often seen in correspondence analysis (CA), DCA records the unimodal response of data to environmental gradients. This simply means a taxon becomes abundant in its preferred ecosystem and gets rarer in stressed conditions (Hill & Gauch, 1980; Hammer et al., 2016). Therefore, taxa appear and disappear along environmental gradients in overlapping sequence. The DCA data are displayed in two dimensions, with two independent axes which account for the major variances in the data set (Figure 3). The magnitude of the variance is measured by the eigenvalue, which determines the percentage variation for each axis.

Within the marine microplankton data sets, there is temporal variation due to the local extinction and appearance of taxa (Usman et al., 2021). Since the microplankton data generated for this study are derived from Cenomanian to Santonian strata, there is a significant stratigraphical repetition of environmental groups. With regard to this, the microplankton data set was divided into two stratigraphical intervals (Yolde-Dukul-Jessu and Sekule-Numanha-Lamja). The microplankton data were pre-filtered to remove statistical variance caused by the inclusion of rare taxa and those with frequencies less than 20 specimens in the total data set. Samples with fewer than five individual microplankton were also removed. The modified data set was composed of 42 samples from the Yolde-Dukul-Jessu interval, and 57 for the Sekule-Numanha-Lamja interval. Each of these was normalised by square root transformation, and these data sets were subjected to DCA using the Palaeontological Statistic 4 (Past) software (Hammer et al., 2016).

In order to determine the impact of sedimentological and geochemical variables on statistically defined microplankton groups (i.e., subsequent to groups being defined by DCA), canonical correspondence analysis (CCA) was undertaken. The CCA method is a modification

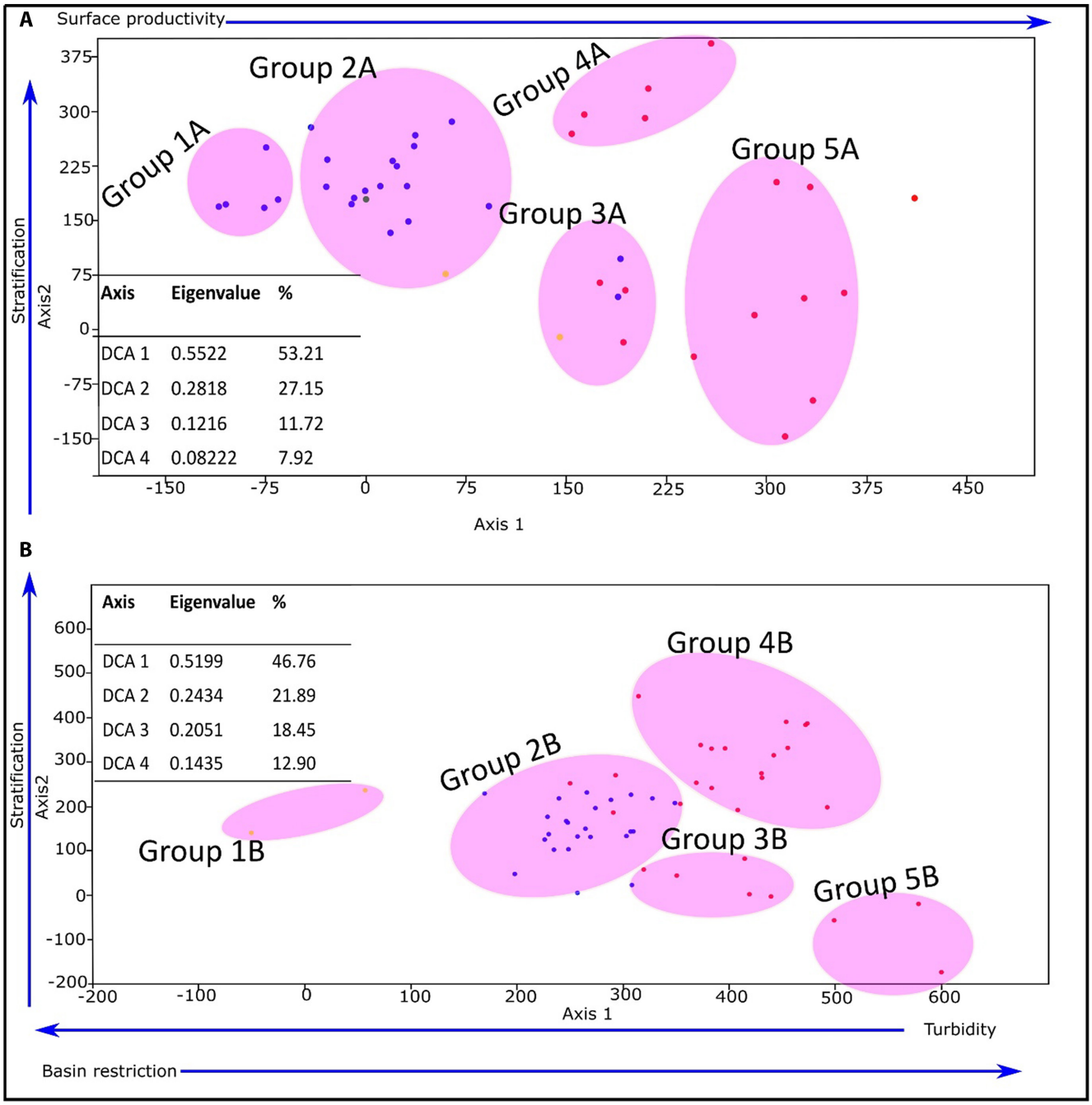

FIGURE 3 Detrended correspondent analysis plot showing taxa distributions. (A) DCA plot for the Yolde-Dukul-Jessu interval. (B) DCA plot for the Sekule-Numanha-Lamja interval. Dots represent palynomorph taxa: algae = yellow dot, microforaminiferal test linings = green dot, gonyaulacoid dinocysts = blue dot and peridinioid dinocysts = red dot. Environmental affinities taxa suggest axis one reflects water circulation and axis two reflects stratification. The eigenvalues for these DCA plots indicate that axis one and two have accounted for 69% or more of the variation within the data set for each.

of weighted averaging ordination that displays species along an explanatory variable. This method has proven useful in understanding species relationships and their responses to environmental variables (Ter Braak, 1986; Palmer, 1993). Two separate analyses were conducted using geochemical (CCA-geochemical) and sedimentological (CCA-sedimentological) explanatory variables. For the CCA-geochemical analysis, the explanatory variables were pXRF data obtained from analysing shale or clay samples. For the CCA-sedimentological analysis, the explanatory variables were derived from numerical values assigned to facies associations. This was achieved by classifying each sample into a particular lithofacies association, and then assigning a numerical value to each lithofacies association. For example, samples obtained from the lower shoreface were all given the same numerical value (here

five), and were represented by zero values in other facies association columns; similarly, an outer shelf facies was ascribed a value of six, with zero for this facies in other facies association columns.

4 | RESULTS

4.1 | Sedimentological results

Photographs of rock outcrops of the formations discussed (Figures 4 through 8) illustrate the variability of lithologies. Twenty-one facies were recognised and described from the Cenomanian–Santonian strata of the Upper Benue Trough (Table 1). These were then grouped into nine facies associations (Table 2). For the limestone strata, eight microfacies were petrographically identified (Figure 9). These facies were deposited in a ramp setting with variable sediment supply. During high siliciclastic input, the sedimentation favours the development of a sand dominated shelf whereas low clastic input favours formation of a carbonate lagoon setting.

4.1.1 | FA1, Outer estuarine tidal bar

This facies association is composed of planar cross-bedded sandstone (Ss2), large scale cross-bedded sandstone (Ss3), small scale cross-bedded to ripple cross-laminated sandstone (Ss4), mud drape sandstone (Ss6) and herringbone cross-stratified sandstone (Ss7) lithofacies. The sandstones are characterised by medium to fine-grained sandstones that are moderately sorted and internally erosive. The large scale trough to planar cross-bedded sandstone is overlain by small scale planar to cross-stratified sandstone (Figure 8B.). It forms large scale herringbone cross-stratification within the thick sandstone units (Figure 8B). The general palaeocurrent directions are to the north-west and south-east, with north-west being dominant. There is an up-section decrease in the thickness of observed sedimentary structures, from large scale trough crossbedding to ripple cross-bedded sandstone. Other sedimentary structures associated with this facies association are tidal bundles and reactivation surfaces. This facies association forms very thick sandstones that range between 5 to 10 m with various superimposed crossbeds. Mud drapes were observed within this facies association, marking the tidal bundles (Figure 6E).

Interpretation

This facies association is interpreted as a tidal bar in an outer estuarine deposit (Boyd et al., 1992; Reynaud & Dalrymple, 2012; Dalrymple, 2010). The large scale crossbeds with well-developed slip faces are interpreted as deposits formed by lateral migration of outer estuarine dunes. In tidal depositional systems, the flood current is more pronounced in seaward areas and the ebb current is more obvious landward (Boyd et al., 1992; Dalrymple et al., 1992; Reynaud & Dalrymple, 2012; Dalrymple, 2010). The planar cross-bedding dipping in the landward and seaward directions, resulting in herringbone cross-stratification, suggests strong ebb and flood tidal currents. The scarcity of claystone deposits associated with this facies association indicates a high energy depositional setting. The erosive bases of units with large scale (70 cm) bidirectional cross-bedding suggest high energy tidal currents (Dalrymple, 2012). Another important structure observed are tidal bundles, which record neap and spring tides. This facies association is interpreted as outer estuarine tidal bar deposits.

4.1.2 | FA2, Estuarine channel

This facies association is characterised by planar and trough cross-bedded sandstone (Ss2), small scale cross-bedded to ripple cross-laminated sandstone (Ss4), mud drape sandstone (Ss6), herringbone cross-stratified sandstone (Ss7), bioturbated sandstone (Ss8), matrix supported conglomerate (Ss10), mudstone (Ms) and shale/clay (Cs) lithofacies. The beds have erosional bases and are internally separated by non-erosional planar surfaces (Figures 8A and 5A). The sediments above the erosive base are characterised by pebbly, mudclast-hosting coarse-grained sandstones. The facies association is generally characterised by fining upward and by decreasing sedimentary structure sizes. The sedimentary structures include trough and planar crossbedding, similar to FA1 (outer estuarine tidal bar) described above. However, this facies association is moderately to highly bioturbated with *Skolithos* and *Ophiomophara* present (Figures 6A,B and 7F). Mud drapes were also observed within the trough cross-bedding of this facies association. Only in a few outcrop sections was herringbone cross-stratification observed although, the palaeocurrent data measured from the sedimentary planar and trough crossbeds indicates bi-directional currents (Figure 3). Figure 8A shows the lateral variation of the sandstone geometry related to the channel migration. The claystone lithofacies associated with this facies association are mostly lenticular, pinkish in colour, and occasionally contain mudcracks.

Interpretation

The erosional-based nature of this facies association suggests deposition in channels. Upward fining indicates deposition under waning flow conditions. The occurrence of the

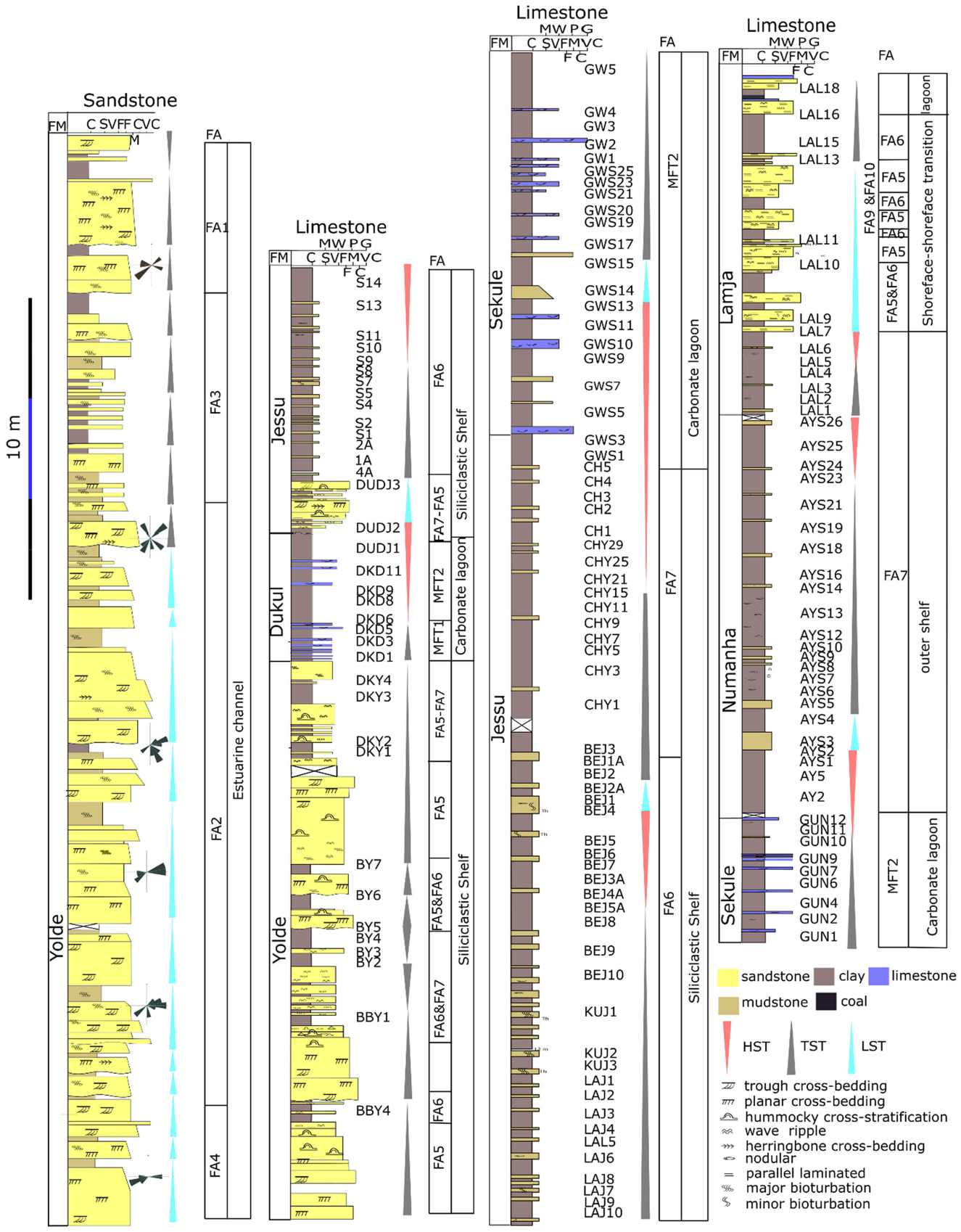

FIGURE 4 A composite lithofacies section of the Cenomanian–Santonian sequences of the Yola Sub-basin with facies associations and depositional sequences. LST (lowstand system tract), TST (transgressive system tract), HST (highstand system tract) and FA (facies association). FA1 (outer estuarine), FA2 (inner estuarine), FA3 (middle estuarine), FA4 (channel), FA5 (shoreface), FA6 (offshore transition), FA7 (outer shelf), MFT1 (lagoon), MFT2 (partially restricted lagoon). The code combining letters and numbers is the sample name (e.g GUN1).

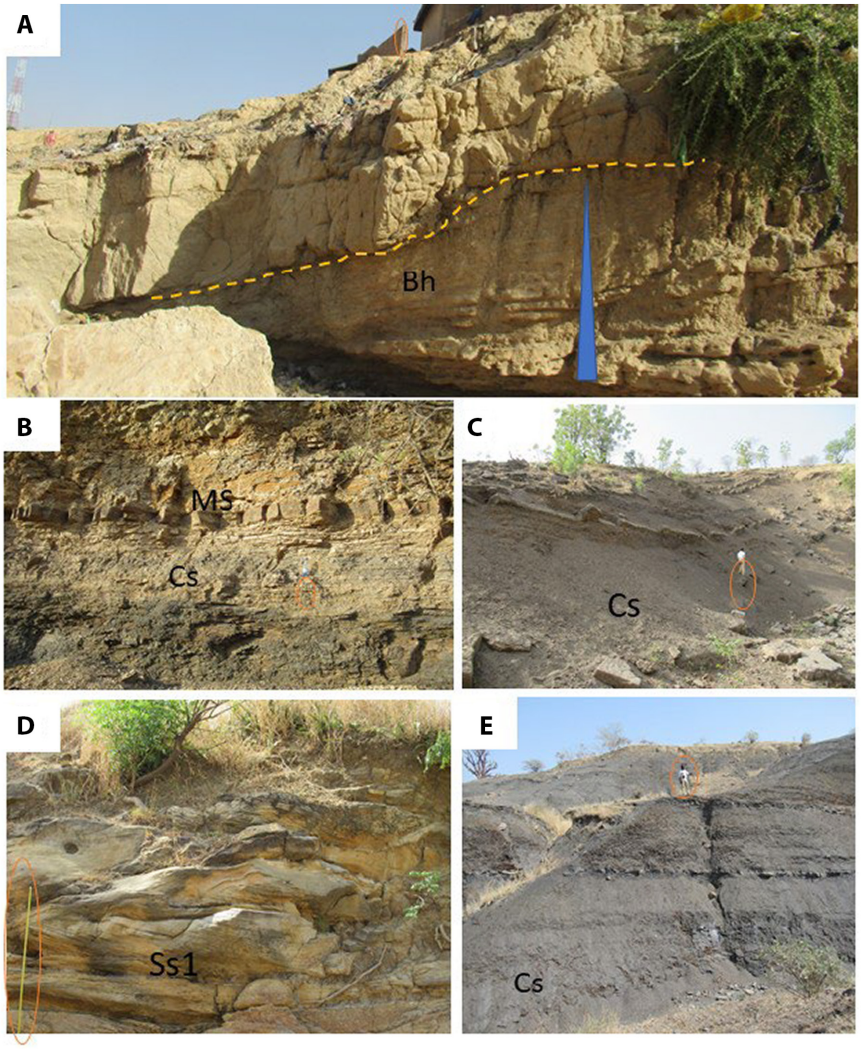

FIGURE 5 (A) Erosional surface at base of estuarine channel and upward fining intertidal facies association, Bh (Heterolithic beds). (B) Mudstone bed (Ms) within grey and dark grey claystone (Cs). (C) Thick brownish to dark grey clay (Cs) with some limestone beds from Sekule Formation. (D) Hummocky cross stratification (Ss1). (E) Dark grey shale with concretional mudstone of Numanha Formation. Scale of each photograph is indicated by a circular ring.

bidirectional and herringbone cross-stratification suggests a tidally influenced environment (Dalrymple & Choi, 2007). The moderate to high bioturbation of this facies association by *Ophiomorpha* and *Skilothos* suggests a subtidal environment (Desjardins et al., 2012). The cross-laminated fine-grained sandstones that are moderately bioturbated are interpreted as deposited in comparatively low energy tidal channels. The presence of mud drapes suggests deposition during the waning stage of the tidal current in estuarine channels. Lenticular clay beds may be related to filling of abandoned channels. This facies association is interpreted as estuarine channel (Clifton, 1982; Miall, 1996).

4.1.3 | FA3, Middle estuary

This facies association, composed of interbedded fine-grained sandstones and clay, contains heterolithic sandstone (Bh), small scale (5 to 15 cm) cross-bedded to ripple cross-laminated sandstone (Ss4), herringbone cross-stratified sandstone (Ss7), parallel laminated sandstone (Ss9), shale/ clay (Cs), and mudstone (Ms) lithofacies. The strata are characterised by lenticular, wavy to flaser bedding that fines and thins upward. The sandstones are characterised by sharp bases and tops, and erosive sandstone beds occasionally occur. The dominant sedimentary structures are ripple cross-lamination and parallel lamination in fine-grained sandstones. Herringbone cross-stratification is rare in this association. However, the palaeocurrent data measured from trough and planar crossbeds indicate bidirectional currents. The deposit shows an increase in clay thickness up section with decreasing thickness of the sandstones (Figure 5A) and bioturbated with *Diplocraterion*. The sandstones are moderately bioturbated with *Skolithos*. The thickness of this facies association can range from 1 to 4.7 m.

Interpretation

The lenticular, wavy to flaser bedding that characterises this facies association indicates deposition under fluctuating hydrological conditions. The observed herringbone cross-stratification and flaser bedding are interpreted as tidal deposits. The finer grain size and planar nature of the beds suggest deposition by low energy currents. The erosively based lenticular sandstones observed are interpreted

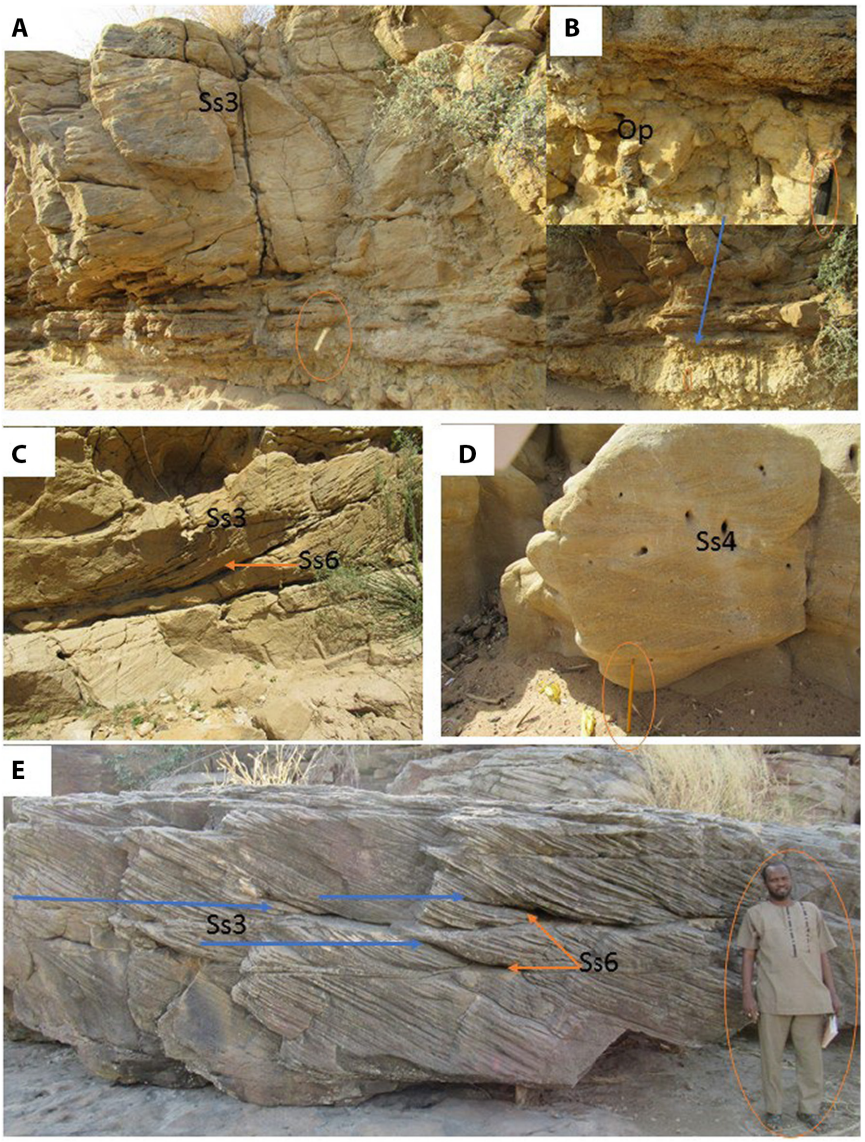

FIGURE 6 (A) Large scale planar cross-bedded sandstone with erosional base overlying a mottled mudstone. (B) Op = *Ophiomorphas* inchofacies. (C) Mud drape within the trough cross-bedded sandstone. (D) Small scale cross-bedded to ripple cross-laminated sandstone. (E) Tidal bundles, blue arrows show different bundle set, SS3 = large scale cross-bedded facies, SS4 = Small scale cross-bedded to ripple cross-laminated sandstones, SS6 = mud drape facies. Scale of each photograph is indicated by a circular ring.

as the result of tidal channel avulsions. The clay deposits may represent deposition within abandoned channels, or middle estuary inter-tidal settings. This facies association is therefore interpreted as middle estuary deposits (sensu Clifton, 1982).

4.1.4 | FA4, Channel

This facies association consists of planar and trough cross-bedded sandstone (Ss2), large scale cross-bedded sandstone (Ss3), small scale to ripple cross-laminated sandstone (Ss4), mud drapes (Ss6), herringbone cross-stratified sandstone (Ss7), shale/ clay (Cs), and mudstone (Ms) lithofacies. It is generally made up of coarse to fine-grained sandstone with pebbly sandstone at the bases of the cycles of upward fining successions. The palaeocurrent direction is dominantly north-west with a subordinate south-east direction. Herringbone cross-stratification and bioturbation are rare in this facies association. Claystones are pinkish and thin. The thickness of this facies association ranges from 1 to 3 m.

Interpretation

The pebbly beds at the base of this facies association are consistent with channel lag deposits. Rare or absent herringbone cross-stratification suggests a depositional environment with little tidal influence (Desjardins et al., 2012; Dalrymple & Choi, 2007). The pinkish colour of the clay might be caused by oxidation of iron. The palaeocurrents are predominantly seaward-oriented, such that they are here interpreted as channel deposits.

4.1.5 | FA5, Shoreface

This facies association is composed of hummocky cross-stratified sandstone (Ss1), planar and trough cross-bedded sandstone (Ss2), small scale cross-bedded to ripple

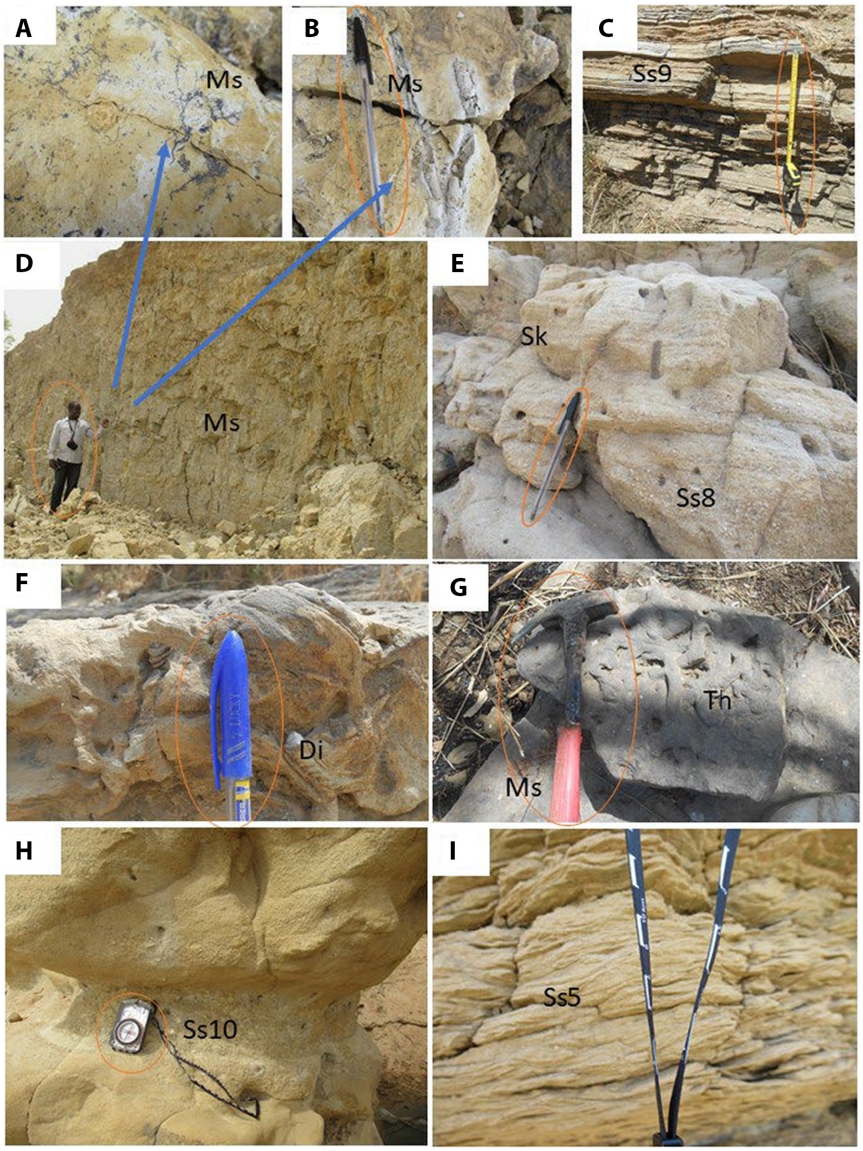

FIGURE 7 (A) (B) and (F) Di = *Diplocraterion* (C) parallel laminated sandstone. (D) mudstone facies. (E) Sk = *Skolithos* (G) Th = *Thallassinoides* on base of a mudstone bed. (H) channel lag. (I) wave ripples, MS = Mudstone facies, SS5 = wave ripple facies, SS8 = bioturbated facies, SS10 = matrix supported conglomerate facies. Scale of each photograph is indicated by a circular ring.

cross-laminated sandstone (Ss4), wave ripple cross-laminated sandstone (Ss5), and heterolithic sandstone (Bh) lithofacies (Figure 5D). The facies association is characterised by coarse to very fine, poor to well-sorted sandstones. Some sandstones have erosive bases with mudclasts and feldspathic gravels. The hummocky cross-stratification grades upward into wave-ripple to parallel-laminated sandstones. The facies association thickness ranges from 0.3 to 2.8 m. Facies association FA5 may be overlain by thick shales forming upward fining successions, or may overlie thick shale forming upward coarsening successions. The upward coarsening successions were recorded in the Yolde, Jessu and Lamja formations, whereas the upward fining trends were only observed in the Yolde Formation.

Interpretation

This facies association is interpreted as shoreface facies, deposited from upper to lower shoreface. Some facies suggest deposition below the fair-weather wave base and above the storm-weather wave base. Hummocky cross-stratification is commonly formed by oscillatory currents between fair-weather base and storm-weather wave base (Dott & Bourgeois, 1982; Dumas & Arnott, 2006). Where this facies association is part of a fining upward sequence it is interpreted as transgressive shelf; when part of a coarsening upward succession it is interpreted as deposited during a regression.

4.1.6 | FA6, Offshore transition

This facies association consists of mudstone (Ms), shale/clay (Cs), heterolithic sandstone (Bh), wave rippled sandstone (Ss5) and parallel laminated sandstone (Ss9) lithofacies. This facies association is characterised by thick clay interbedded with fine-grained sandstones and mudstones. The mudstones are bioturbated with *Thalassinoides*, *Planolites*, *Rhizocorallium* observed, and they contained a lot of organic

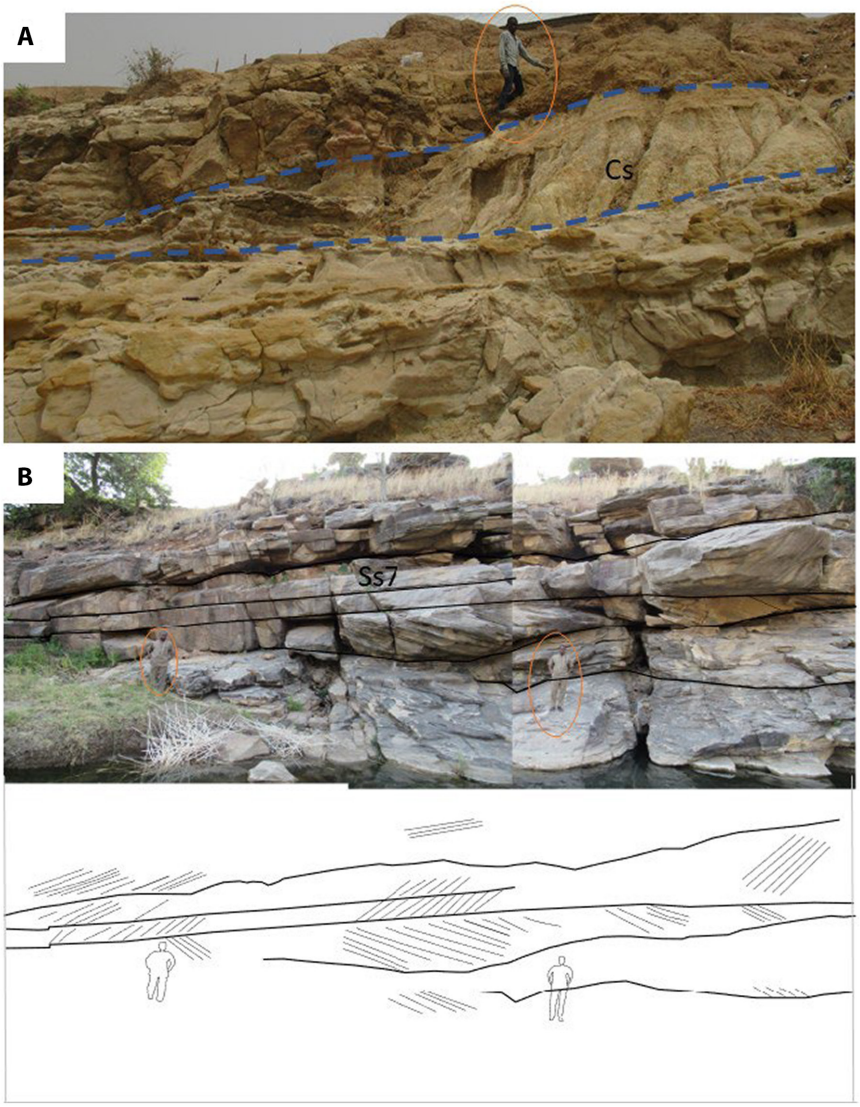

FIGURE 8 (A) Lateral lithofacies variations within tidal channel facies succession. (B) Subtidal facies association with herringbone cross bedding and erosional surfaces; SS7 = herringbone cross-stratified. Scale of each photograph is indicated by a circular ring.

matter. The *Thalassinoides* burrows are mostly observed on the sole of the mudstone beds. The mudstone varies in thickness from 30 cm to 1.7 m. This facies association itself is up to 50 m in thickness (Figure 3). This facies association is common in the Yolde, Jessu and Lamja formations.

Interpretation

This facies association suggests deposition in a muddy shelf environment. The muds may have been moved to deeper waters by re-suspension due to wave currents on a shallow, gently sloping shelf (Plint, 2010). The bioturbation suggests an oxygenated depositional setting. This facies association is interpreted to have formed in offshore transition environments.

4.1.7 | FA7, Outer shelf

This facies association consists of parallel laminated sandstone (Ss9), mudstone (Ms) and shale /clay (Cs) lithofacies. It is characterised by thick shale or clay with thin, fine-grained sandstone and mudstone deposits. The sole of the mudstone is occasionally bioturbated with *Thalassinoides* observed (Figure 6H). The shales are grey and vary in thickness from 0.7 to 40 m.

Interpretation

This facies association is interpreted as offshore marine deposits, formed in a relatively quieter water body than the shallower facies, which allowed suspension settling or fall out of finer particles (Varban & Plint, 2008; Plint, 2010).

4.1.8 | MFT1, Lagoon

This facies association is composed of bivalve packstone (M1), gastropod-bivalve packstone (M2), gastropod packstone (M3), and bivalve wackestone (M6) microfacies. The gastropods and some bivalves have been dissolved and

TABLE 1 Lithofacies description and interpretations of the Cenomanian–Santonian strata. HCS = Hummocky Cross-Stratification; TXB = trough cross-bedding; PXB = planar cross-bedding; LMC = low magnesian calcite.

Lithofacies	Description	Bioturbation	Interpretation
Ss1	Hummocky cross-stratified sandstones (Figure 5D) Very fine to fine-grained sandstones, with 0.25 to 0.5 m thick HCS sets., Thicknesses from 0.25 to 2.5 m. Some erosional surfaces with flaser clay	Rarely bioturbated	Deposition between fair-weather wave base and above a storm-weather wave base
Ss2	Medium scale cross-bedded sandstones Coarse to medium grained sandstones with PXB and TXB. Units from 0.6 to 2.8 m thick. Lithofacies has a bidirectional palaeocurrent	Mostly bioturbated by *Skolithos*	Formed by migration of 2D and 3D dune
Ss3	Large scale cross-bedded sandstones (Figure 6A,C,E) Medium grained sandstone with *ca* 1 m cross stratification set with a planar base	Rarely bioturbated	Formed by lateral migration of large point bar or dunes.
Ss4	Small scale cross-bedded to ripple cross-laminated sandstones (Figure 6D) Fine to medium grained sandstones, co-sets range from 0.1 to 0.5 m. thick. Bidirectional palaeocurrents. Individual units 3 to 4 cm thick	Occasionally bioturbated with *Skolithos*, *Ophiomorphar*	Formed by migration of small dune
Ss5	Wave rippled cross-laminated sandstones (Figure 7I). Occurs in very fine to fine-grained sandstones, from 0.05 to 1 m thick	Occasionally bioturbated	Formed by wave activities in marine environments
Ss6	Mud drape sandstone (Figure 6C,E) Fine to medium grained sandstones with 1 to 2 cm thin mud in TXB sandstones. Cross beds show bidirectional current. Foresets from 0.3 to 0.6 m thick, North-east oriented palaeocurrent direction common	Rarely bioturbated	Formed during slack water period in tidal environments
Ss7	Herringbone cross-stratified sandstones (Figure 8B), fine to medium grained sandstone with planar or erosional base. Units from 0.2 to 2 m thick	Occasionally bioturbated	Formed by migration of ebb and flood dunes in tidal environments
Ss8	Bioturbated sandstones (Figure 7E,F) Very fine to fine-grained sandstone. Unit ranges from 0.5 to 1 m thick; rare sedimentary structures	Highly bioturbated with *Diplocraterion*, *Rhizocorallium* and *Skolithos*	Deposition in areas with low sedimentation rate
Ss9	Parallel laminated sandstones (Figure 7C) Silty to very fine-grained sandstones, thinly laminated often ripple cross laminated. Beds have planar bases, occasionally bioturbated with vertical burrows	Occasionally bioturbated	Deposition in low energy environments with fluctuating hydrological conditions.
Ss10	Matrix supported conglomerate (Figure 7H) Gravel to very coarse-grained sandstone. Thicknesses from a few cm to 0.4 m. Gravels comprise mud clasts within coarse to medium grained sandstone matrices	Absent	Deposition at the base of channel
Bh	Heterolithic beds (Figure 5A) Thin beds of very fine-grained sandstone interbedded with siltstones or mudstones. Flaser clay and lenticular bedding. Sandstone includes ripple and parallel laminations. Unit ranges from 0.6 to 3 m thick	Moderately bioturbated with Skolithos	Deposition in environment with fluctuating hydrodynamic conditions
Ms	Mudstone (Figure 7D,G) Clay to siltstone beds 0.1 to 2.3 m thick	Absent to sparse Thalassinoides observed at base of beds. Some highly bioturbated with unidentified inchnofacies.	Storm generated deposits into deeper or shallower low energy outer shelf environments

(Continues)

TABLE 1 (Continued)

Lithofacies	Description	Bioturbation	Interpretation
Cs	Claystone (Figure 5B,C,E) unit ranging from a few cm to 40 m thick	Rarely bioturbated, however, some are bioturbated at the surface by Thalassinoides	Fallout in quite water environments
M1	Bivalve packstone (Figure 9A) Limestone with articulated and disarticulated bivalves plus bryozoans. Aragonite subsequently replaced by ferroan calcite		Fauna indicates shallow marine, and ferroan calcite suggests low oxygen (restricted lagoon?).
M2	Gastropod-bivalve packstone (Figure 9B,C) Bivalves and gastropods, with.gastropods replaced by ferroan low magnesian calcite. Chambers filled with phosphatic material and poorly sorted		Shallow marine, low oxygen, restricted?
M3	Gastropod packstone (Figure 9E) Dominantly gastropods in a non-ferroan calcite matrixShells altered to ferroan LMC Also bivalve fragments and peloids, poorly sorted		Shallow marine, low oxygen, restricted, with micrite producers (presumed green algae?)
M4	Phosphatic peloids (Figure 9F,G) Wackestone-packstone dominated by phosphatic intraclasts. Allochems include gastropods, ostracods and Fusulinid foraminifera. Gastropod and ostracod chambers filled with phosphate. Phosphatic intraclasts also include peloids		Phosphate of faecal origin, in a shallow marine, restricted and perhaps slightly hypersaline lagoon?
M5	Ostracod Packstone: (Figure 9J,K) Ostracod bioclasts in micritic matrix that ranges from ferroan to non-ferroan calcite. Ostracods include many that are articulated, with some disarticulated fragments. Also bivalve shells and phosphatic peloid intraclasts, poorly sorted		hypersaline lagoon?
M6	Bivalve wackstone: (Figure 9D) Ferroan calcite micrite with bivalve shell fragments, echinoid spines, cephalopods, ostracoids and peloids, poorly sorted		Shallow marine, generally open marine but ferroan calcite suggests periodically restricted?
M7	Bryozoan packstone: (Figure 9H,I) Bryozoan wackstone-packstone. Bryozoan zooecia filled by sparry calcite while zooecia wall comprises slightly ferroan to non-ferroan calcite. Associated with non-ferroan calcite bivalve shell		Deposition in relatively open shallow marine environment

the spaces the shells occupied have been filled with calcite cement. Using Dunham's classification of limestone (Dunham, 1962), the facies is classified as packstone to wackestone, while based on Folk's classification scheme it is considered to be a biomicrite (Folk, 1959) (Figure 9A through D).

Interpretation

The presence of gastropods and bivalves is consistent with shallow (*ca* 1 to 10 m?) lagoonal environments with seagrasses on which the gastropods would likely feed. Fragmented shells suggest some re-working in waters that were agitated by waves and storms.

4.1.9 | MFT2, Lagoon

This facies consists of ostracod packstone (M5), bivalve wackstone (M6), phosphatic peloid (M4), bryozoan packstone (M7) microfacies. Other fossils such as sponges, echinoids, calcispheres, miliolid foraminifera and ostracods were observed. The bryozoans were preserved as whole-body fossils with the inner zoacia being filled with spar calcite whiles the outer wall is made up of non-ferroan calcite and is associated with bivalve shells. The bivalve wackestone is dominated by micrite, with bivalves and phosphatic peloid grains. The gastropods are not well preserved because the original

TABLE 2 Facies association derived from the lithofacies.

Facies association	Lithofacies	Description	Interpretation
FA1	Ss2, Ss3, Ss4, Ss6 and Ss7	Comprises very thick internally erosive amalgamed sandy units. Large scale cross bedding with tidal bundles and mud drapes recording strong ebb and flood tides. Palaeocurrent directions NW-SE. Rarely bioturbated. c. 10 m thick, grading into flaser bedded sandstones (Figure 8B)	Deposition in outer estuarine channels or tidal bar
FA2	Ss10, Ss2, Ss4, Ss6, Ss7, Ss8, Ss10, MS and Cs	Bioturbated cross -stratified sandstones and clay to mudstone deposits. Bidirectional palaeocurrents, dominantly NE. Characterised by an erosive base with pebbles, mudclasts, and generally upward fining. Ichnofacies included in this facies association are *Skilothos* and *Ophiomorpha*. This facies association consists of geometrically lenticular claystone. (Figure 8A)	Deposition in inner estuarine channels
FA3	Bh, Ss4, Ss7, Ss9, and Ms	Planar parallel laminated and ripple cross-bedded thin beds of fine-grained sandstone interbedded with siltstone to mudstones (Figure 4A). Shows general fining and thinning upward. Small scale herringbone cross stratificationsobserved within very fine to fine-grained sandstones. Moderately bioturbated	Deposition in fluctuating hydrological conditions probably intertidal or central estuarine
FA4	Ss10, Ss2, Ss4, Ss6, Ss7, Ss8, Ss10, Ms and Cs	Upward fining facies association with coarse to fine-grained sandstone capped by pinkish mudstone. Rarely bioturbated with dominant SW palaeocurrent direction, and subordinate NE direction (Figure 4)	Deposition in channels
FA5	Ss1, Ss2 Ss1 Ss5, Ss4, SS10, Csand Bh	Medium to fine-grained planar and trough cross-bedded sandstone with erosional base, wave ripples and HCS (Figure 5D); occasionally bioturbated with *Thalassinoides Rhizocolallium*, *Skolithos* and *Planolites*. In places upward fining, and in others upward coarsening	Deposition in regressive-transgressive high energy marine environments probably shoreface
FA6	Ms, Cs, Bh, Ss5 and Ss9	Heterolithic parallel laminated sandstone mudstone and claystone. Mudstone units from 30 cm to 1.7 m thick. Facies association ranges from 1 to 50 m thick (Figure 4)	Deposition in offshore transition environment
FA7	Ss9, Ms and Cs	Dominantly thick shale with mudstone and marlstones (Figure 5B,E). Some mudstone beds nodular with bivalves,occasionally bioturbated with *Thalassinoides*	Deposition in quiet water environment with episodic storm in outer shelf environment
MFT1	M1, M2, M3, and M6	Limestones, poorly sorted to moderately sorted, with bioclasts of bivalves and gastropods. Gastropods dissolved and moulds filled with non-ferroan calcite. Micrite may be ferroan	The facies association suggests deposition in shallow agitated environments and its interbedding with clay suggest agitated water environment. The facies association indicates lagoon environment
MFT2	M5, M6, M4, and M7	Poorly sorted microfacies that consists of dominantly ostracods, phosphatic peloid, bryozoan and other subordinate bioclast. The phosphatic peloids are angular to rounded	The facies association suggest deposition in less agitated partially restricted lagoon environments

aragonite has been replaced by calcite. Poorly sorted fragmented and articulated ostracods were observed within the microfacies. The limestone beds are grey in colour and some are bioturbated by *Thalassinoides* at their base (Figure 7G).

Interpretation

Ostracods, sponges and miliolid foraminifera are all consistent with lagoonal waters that may have been partially restricted. Bryozoans are exclusively marine but are known to occur in brackish marine to normal marine depositional environments (Flügel, 2010). The bivalve wackestones with bryozoans in micrite are also consistent with deposition in a shallow, protected environment. Phosphatic peloids can have several origins, although they can indicate high biological productivity at the sediment: water interface under low oxygen conditions (Arning et al., 2009). The occurrence of phosphates precipitated inside gastropod shells and ostracod tests, and laminated phosphate in the limestone and its occurrences within thick shale, suggests deposition in a restricted lagoonal environment. The presence of ammonites indicates that there was a marine connection, such that the lagoon was partially, but not fully, restricted.

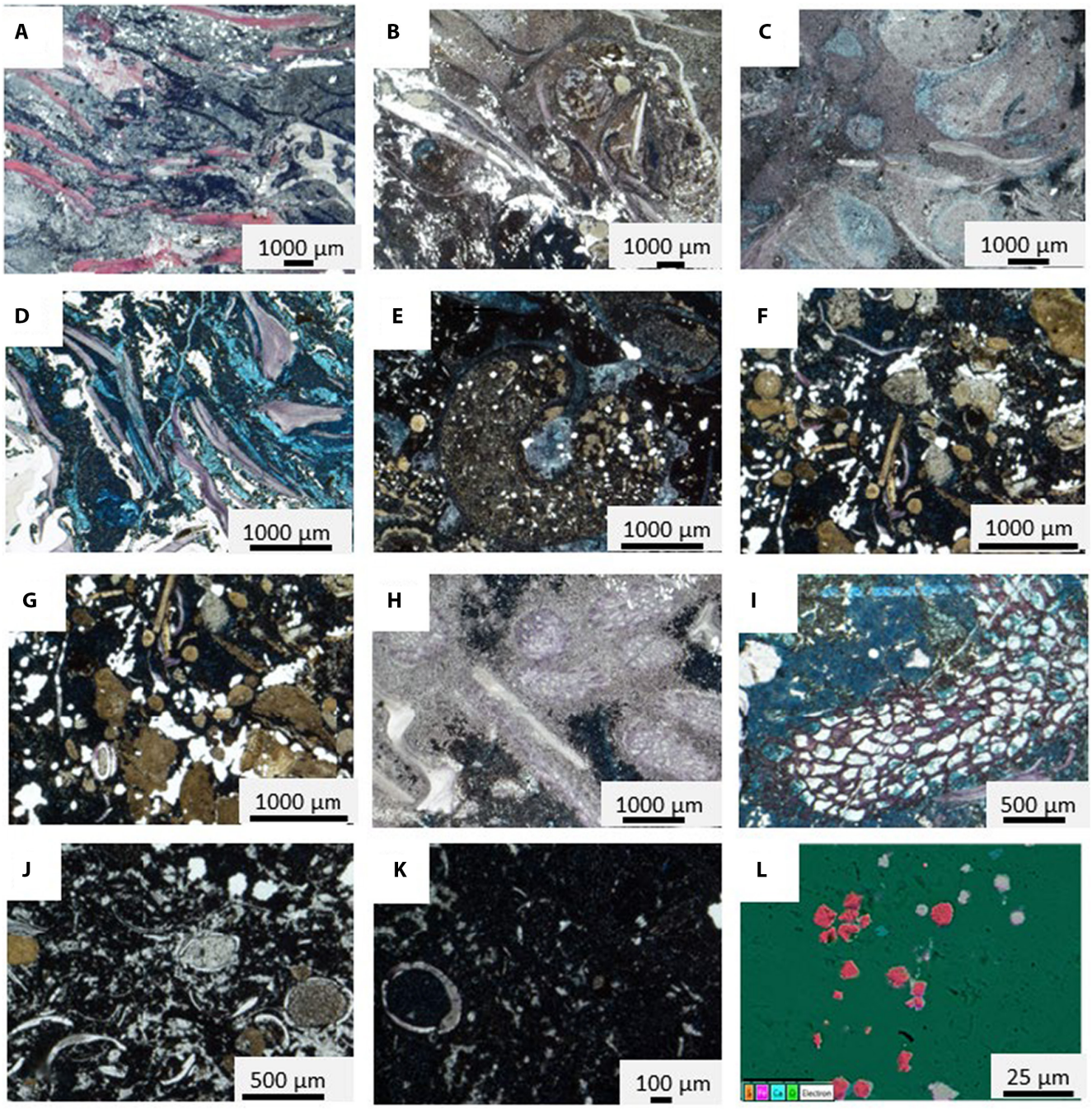

FIGURE 9 (A) Bivalve packstone, with fragmented and altered bivalves. (B) Bivalve and altered gastropod packstone. (C) Gastropod packstone. (D) Bivalve wackestone-packstone. (E) gastropod mould filled with phosphate (F) and (G) Intraclastic peloid packstone-wackstone. (H) and (I) Bryozoan bivalve packstone. (J) Ostracod packstone-wackstone. (K) Ostracod mudstone-wackestone. (L) Framboidal pyrite. Scale of each photograph is indicated by a scale bar.

4.2 | Palynological results

Preservation of palynomorphs from Cenomanian–Santonian rocks was moderately good. The Yolde and Dukul formations yielded few dinocysts, but diversity increased up section. Dinocyst floras from these formations are dominated by peridinioid taxa with subordinate gonyaulacoid species. Assemblages recovered from the overlying, younger formations are composed of variable proportions of peridinioid and gonyaulacoid dinocysts, Chlorophyceae and microforaminiferal test linings.

Palynological analysis of 136 samples yielded 135 dinocyst taxa in association with other algae and microforaminiferal test linings (e.g. Plates 1, 2 and see Usman et al., 2021). Microplankton assemblages from the Cenomanian–Santonian strata of the Upper Benue Trough show variation within the sections (Figures 10 and 11). Shale-dominated intervals exhibit higher

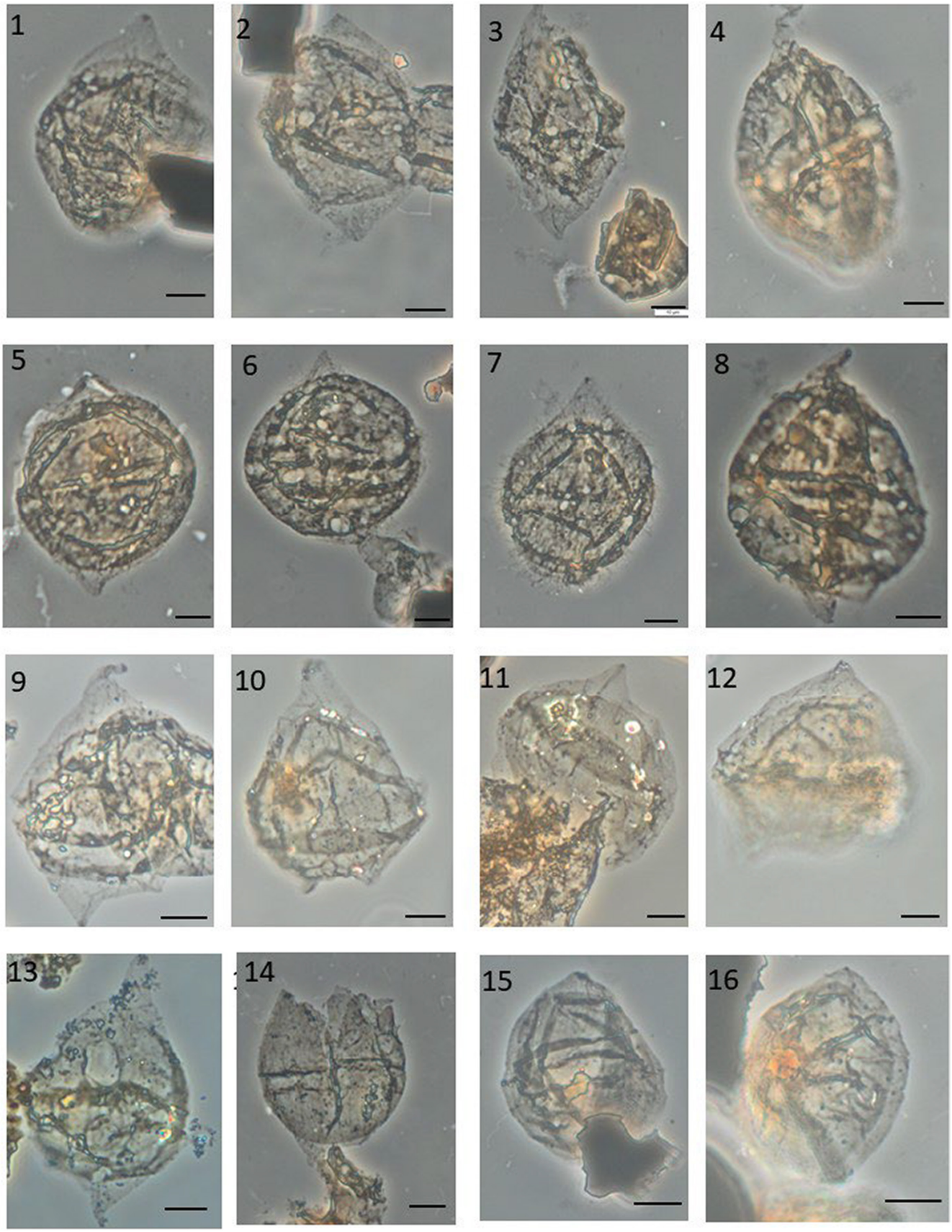

PLATE 1 Selected microplankton from Yola Sub-basin, scale bar represents 10 μm. 1,2, *Subtilisphaera perlucida*, samples DKD5 D36/3 and DKD5 D40/4. 3,4, *Subtilisphaera pirnaensis*, samples DKD5 D36/0 and E38/0. 5,6, *Subtilisphaera senegalensis*, sample DKD5 C57/0. 7, *Palaeohystrichophora infusorioides*, sample DKD5. 8, *Subtilisphaera zawia*, sample DKD5. 9, *Isabelidinium glabrum*, sample AYS25, P57/1. 10, *Isabelidinium acuminatum*, sample S7. 11,12, *Palaeoperidinium* sp., sample S7. 13, *Alterbidinium* sp. cf. *asymmetricum* Wilson, 1967a, sample AYS23, G38/0. 14, *Ovoidinium* spp., samples AYS25 D52/2 and GUN2. 15,16, *Eurydinium ingramii*, sample S11 G49/0, K37/1.

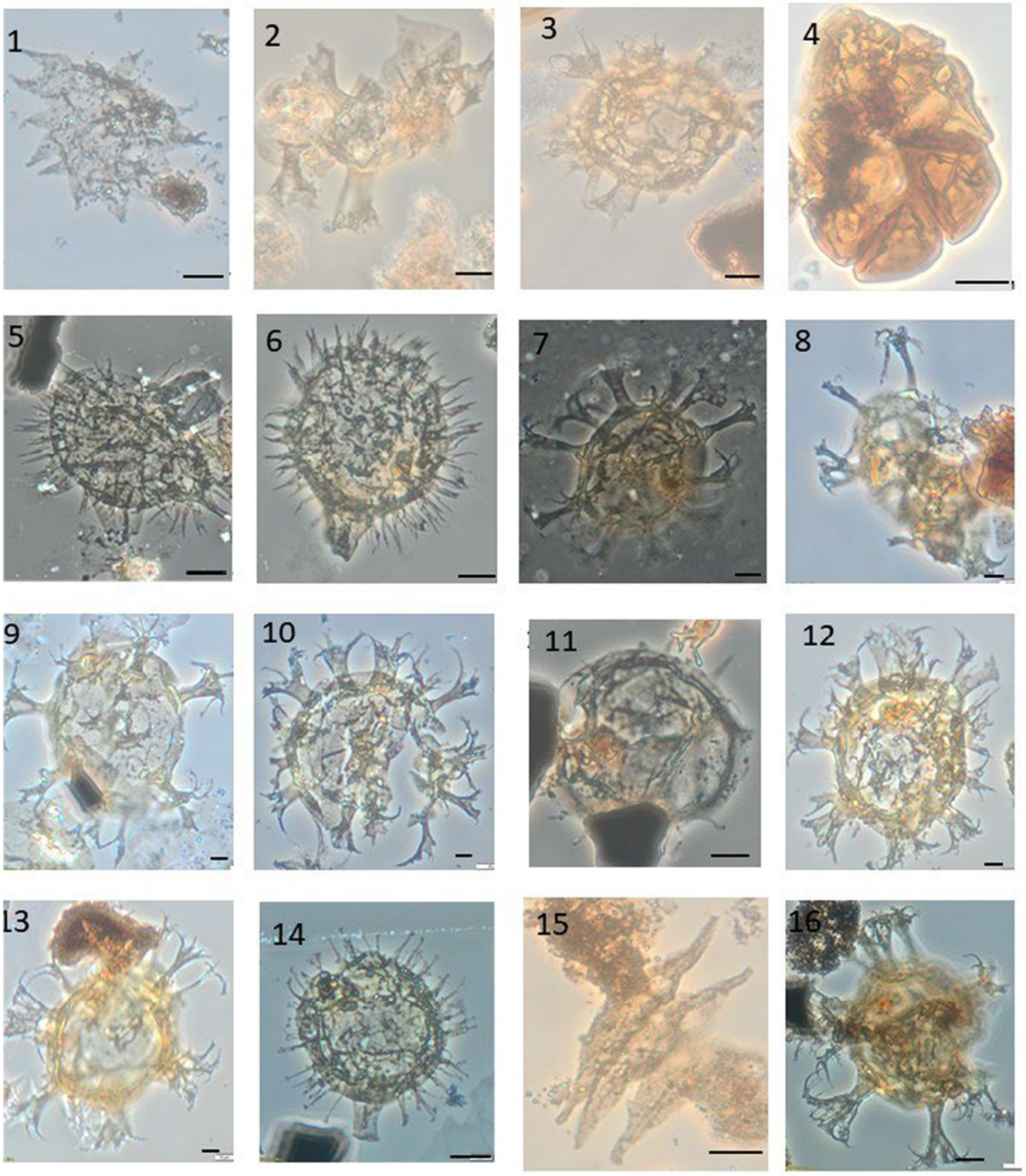

PLATE 2 Selected microplankton from Yola Sub-basin, scale bar represents 10 μm. 1, *Pediastrum bifidus*, sample S5. 2, *Oligosphaeridium albertense*, sample GUN9. 3,4, *Oligosphaeridium asterigerum*, sample GUN4. 4, *Microforaminiferal test linings*, sample S5. 5, *Florentinia clavigera*, samples LZN4. 6, *Florentinia laciniata*, sample CH4. 7,8, *Oligosphaeridium complex*, sample LZN4 U26/2 and GW6 B46/4. 9,10, *Oligosphaeridium irregulare*, sample GW6 K47/4 and B47/3. 11, *Trichodinium castanea*, sample AYS18. 12,13, *Oligosphaeridium perforatum*, Gocht 1959 samples GW6 D35/4 and LZN4 X28/0. 14, *Coronifera oceanica*, samples AYS23 Q30/2. 15, *Scenedesmus* sp., sample S5. 16, *Oligosphaeridium pulcherrimum*, sample AYS23.

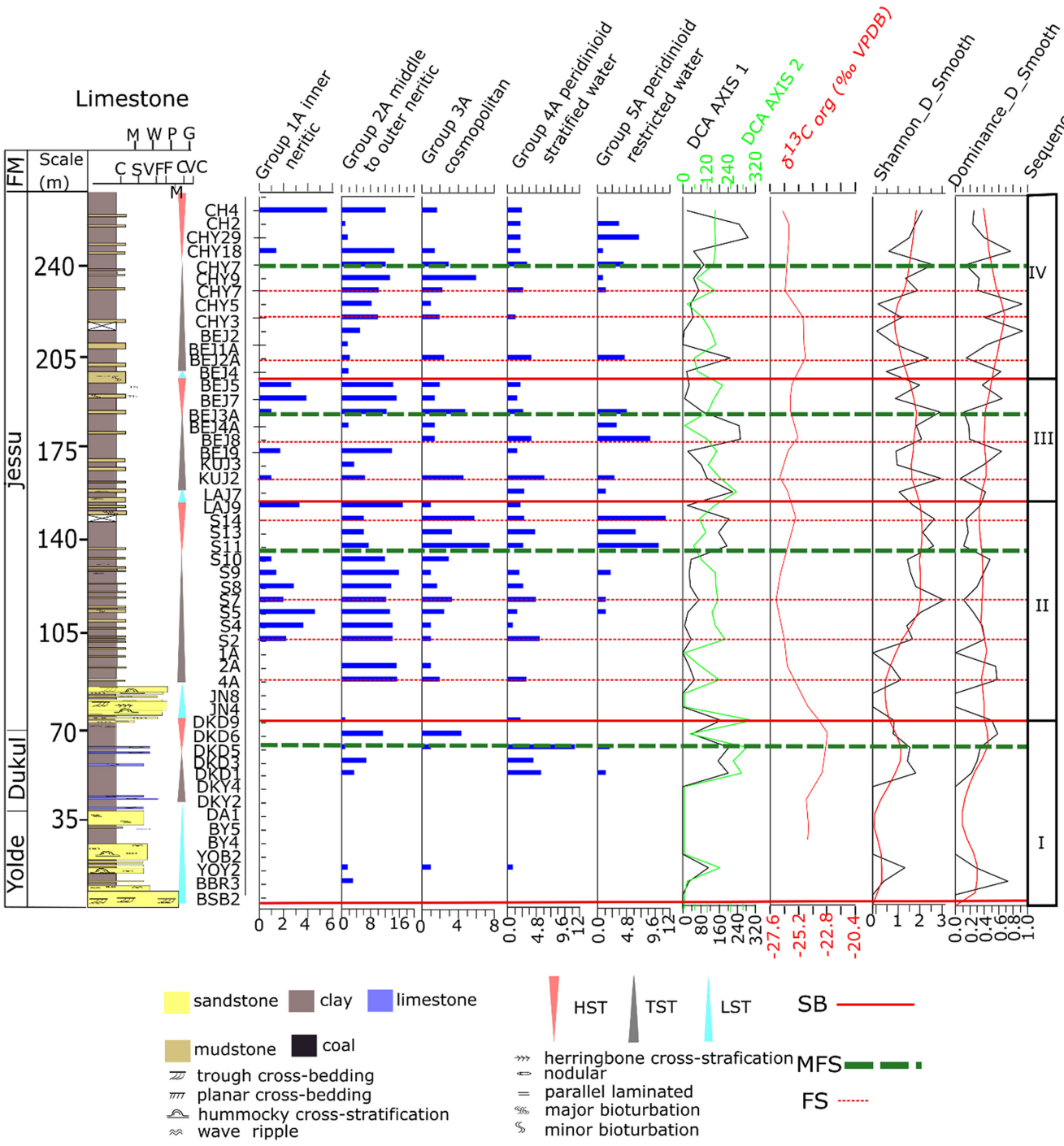

FIGURE 10 Showing stratigraphical distribution of the DCA groups, DCA axes, Shannon diversity index, dominance diversity index and sequences (seq.) identified for the Yolde-Dukul-Jessu interval. Axis one reflects open marine and restricted marine whereas axis two reflects turbidity. Microplankton diversity index and microplankton dominance index represented by grey line with red smooth averaging line.

abundances of microplankton than do the sand-dominated intervals. This could be due to a taphonomic issue that oxidised the microplankton, leading to low preservation of organic matter. It could also be explained by the ecological stress conditions associated with high turbidity in sand-dominated depositional environments.

Ecological analyses show that shale-dominated intervals exhibit a higher Shannon diversity index than those from arenaceous intervals (Figures 10 and 11). In contrast, the dominance index is higher in arenaceous strata than in argillaceous strata. Low values for the dominance index (≤0.3) indicate that the microplankton are evenly distributed, whereas a high dominance index (≥0.7) value suggests a few taxa are dominant over the others in the sample.

For the Yolde-Dukul-Jessu interval, the DCA result clustered into five distinctive statistical groups (Table 3),

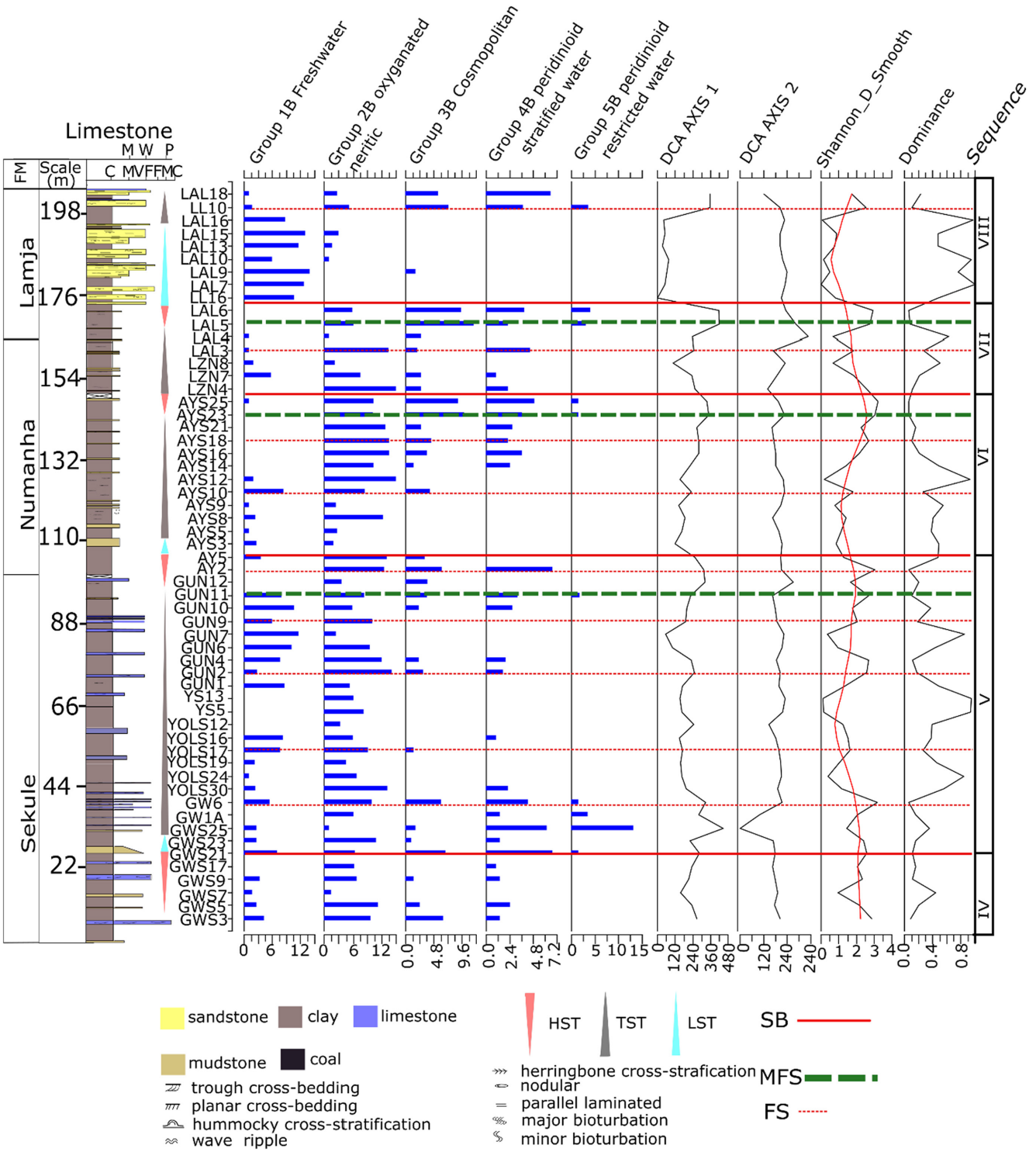

FIGURE 11 Stratigraphical distribution of the DCA groups, DCA axes, Shannon diversity index, dominance diversity index and sequences (seq.) identified for the Sekule-Numanha-Lamja interval.

two gonyaulacoid-dominated, and three peridinioid-dominated microplankton groups. The distance between groups one and five is more than four standard deviations (SD), and importantly the two DCA axes accounted for 80.36% of the variation within the data set (Figure 3A). For the Sukule-Numanha-Lamja interval the DCA results are clustered into five groups, namely: algae, three peridinioid dinocyst groups, and gonyaulacoid dinocysts and microforaminiferal test linings group. The distance between the end-member clusters is approximately four standard deviations, and the two DCA axes accounted for 68.65% of the variation within the dataset (Figure 3B).

TABLE 3 List of microplankton groups obtained from DCA of the Dukul-Jessu interval and Sekule-Numanha-Lamja intervals.

Palynomorphs Communities of the Yolde-Dukul-Jessu interval	
Group 1A (Inner neritic)	**Group 3A** (Cosmopolitan)
Florentinia berran	*Scenedesmus* sp.
Florentinia clavigera	*Cribroperidinium edwardsii*
Xenascus plotei	*Alterbidinium* sp.
Florentinia resex	*Ascodinium* sp.
Coronifera cf. c. *oceanica*	*Ovoidinium* sp
Group 2A (Middle to outer neritic)	*Apteodinium* Eisenack 1958
Microforaminiferal test linings	**Group 4A** (Peridinioid stratified)
Cleistosphaeridium spp.	*Palaeohystrichophora infusorioides*
Cyclonephelium distinctum	*Palaeohystrichophora cheit*
Florentinia khaldunii Below 1982	*Subtilisphaera pirnaensis*
Spiniferites lenzii	*Subtilisphaera perlucida/deformas*
Achomosphaera triangulata	*Subtilisphaera senegalensis*
Cyclonephelium vannophorum	**Group 5A** (Peridinioid restricted)
Cyclonephelium compactum	*Eurydinium eyrense*
Protoellipsodinium clavulus	*Eucladinium madurense*
Coronifera oceanica	*Subtilisphaera* sp.
Exochosphaeridium bifidum	*Deflandrea* sp
Downiesphaeridium sp.	*Manumiella druggii*
Prolixosphaeridium deirense	*Cribroperidinium aceras* (Eisenack, 1958)
Florentinia radiculata	*Eurydinium ingramii*
Prolixosphaeridium parvispinum	*Senegalinium* sp1
Pediastrum bifidus	*Ovoidiniun* sp.2
Implestosphaeridium clavus	
Achomospheara neptuni	
Palynomorphs assemblages of the Sekule-Numanha-Lamja interval.	
Group 1B (Freshwater)	**Group 3B** (Cosmopolitan)
Pediastrum bifidus	*Alterbidinium earnleyense*
Scenedesmus sp.	*Isabelidinium gabra/ belfastense*
Group 2B (Oxygenated neritic)	*Paleohystrichophora infusorioides*
Microforaminiferal test linings	*Manumiella druggi*
Cleistosphaeridium spp	*Palaeoperidinium* sp.
Cyclonephelium distinctum	*Downiesphaeridium* sp.
Achomosphaera verdieri	**Group 4B** (Peridinioid stratified)
Florentinia berran	*Eucladinium madurense*
Exochosphaeridium bifidum sensu Below 1982	*Andalusiella polymorpha (*Malloy, 1972*)*
Florentinia radiculata	*Cribroperidinium edwardsii*.
Florentinia khaldunii Below 1982	*Deflandrea* sp. 2
Subtilisphaera pirnaensis	*Deflandrea* sp.1
Achomosphaera danica	*Alterbidinium* sp.
Implestosphaeridium clavus	*Deflandrea* sp.6
Florentinia clavigera	*Senegalinium* sp.2
Achomosphaera triangulata	*Deflandrea* sp. 7
Achomosphaera neptuni	*Alterbidinium* sp. A
Cyclonephelium vannophorum	*Ovoidinium* sp.
Hystrichodinium sp.cf. *H. pulchrum*	*Cribroperidinium* sp.
Cyclonephelium compactum	*Eucladinium gambangense*
Subtilisphaera perlucida/deformas	*Isabelidinium seelandica*
Coronifera oceanica	*Paleohystrichophora cheit*
Oligosphaeridium pulcherrimum	*Senegalinium* sp.1
Downiesphaeridium armatum	*Florentinia resex*
Spiniferites lenzii	**Group 5B** (Peridinioid restricted)
Trichodinium castanea	*Eurydinium ingramii*
Subtilisphaera senegalensis	*Manumiella eyrenseare*
Oligosphaeridium irregulare	*Manumiella* sp. 1

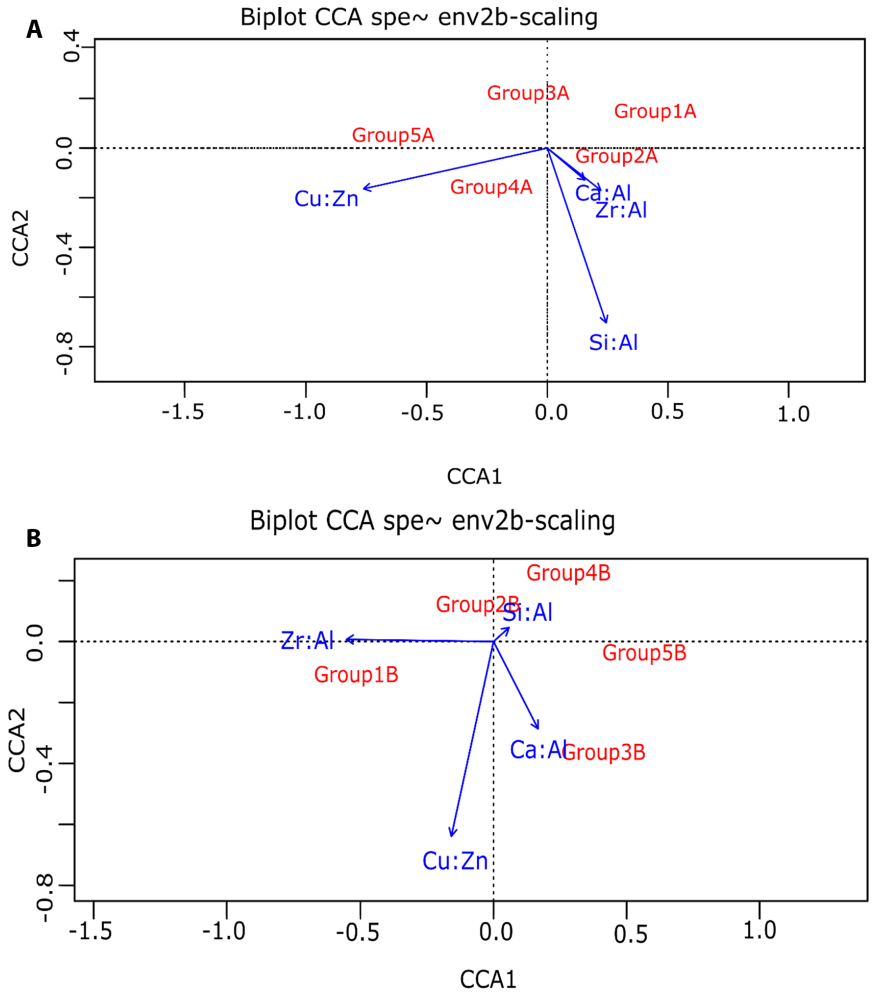

FIGURE 12 CCA plot with geochemical data as environmental variables and DCA palaeoecological communities as response variable for the Yolde-Dukul-Jessu interval (A) and Sekule-Numanha-Lamja interval (B). The blue lines and their labels indicate the environmental variables while the groups are taxa assemblages. The positive correlation with Zr:Al ratio suggests increase in heavy mineral content, Si:Al ratio represents abundance of the clay component component, Cu:Zn ratio as a proxy of reduced conditions and Ca:Al ratio as likely reflection of increase in carbonate content.

Despite the different depositional settings for the Yolde-Dukul-Jessu and Sukule-Numanha-Lamja intervals, DCA derived groups (Figure 3A,B) show a similar compositional distribution. This can be interpreted as the same environmental controls applying to both stratigraphic intervals. In an attempt to understand the key environmental controls on the data, the microplankton ecological groups identified from DCA were compared with facies associations or geochemical variables. These are the environmental variable used in CCA (Figures 12 and 13). The CCA data show each microplankton group correlated with a different variable.

4.3 | Geochemical results

An pXRF analysis of shale samples yielded concentrations of Mg, Al, Si, P, S, K, Ca, Ti, Mn, Fe, Ni, Cu, Zn, As, Rb, Sr, Y, Zr, Nb, Pb and Th. The measured concentrations of these elements could be proxies for environmental variables that could then be linked to microplankton group data. The CCA results indicate that Al, Si Ca, Fe, Cu, Ti and Zr have high statistical significance factors.

Elevated concentrations of Si, Ti, Zr and Rb might suggest influxes of heavy minerals. However, the concentrations of these elements can be modified by diagenesis. To reduce the effect of diagenesis on interpretations, the elements were normalised with Al, which is considered relatively immobile during diagenesis (Bloch, 1998). Zirconium is commonly derived from heavy minerals, such that the Zr:Al ratio likely reflects increased abundance of heavy minerals. Copper and Zinc sulphides have different solubility in reducing and oxidising conditions (Hallberg, 1976), as the precipitation of Cu is enhanced under reducing conditions in comparison to Zn. Because of this, the ratio of Cu and Zn can be used as a proxy to determine reducing depositional environments (Hallberg, 1976). The ratio of Ca to Al could reflect an increased carbonate component, although this may also be linked with diagenetic cements. The ratio of Si to Al may reflect the balance between quartz, clays and feldspars.

These ratios were used as variables for the microplankton groups for CCA. The results of the CCA undertaken here indicate that increased Zr:Al ratios are associated with microplankton group 1B, whereas an increase in Si:Al ratios suggests an influence on the peridinioid-dominated

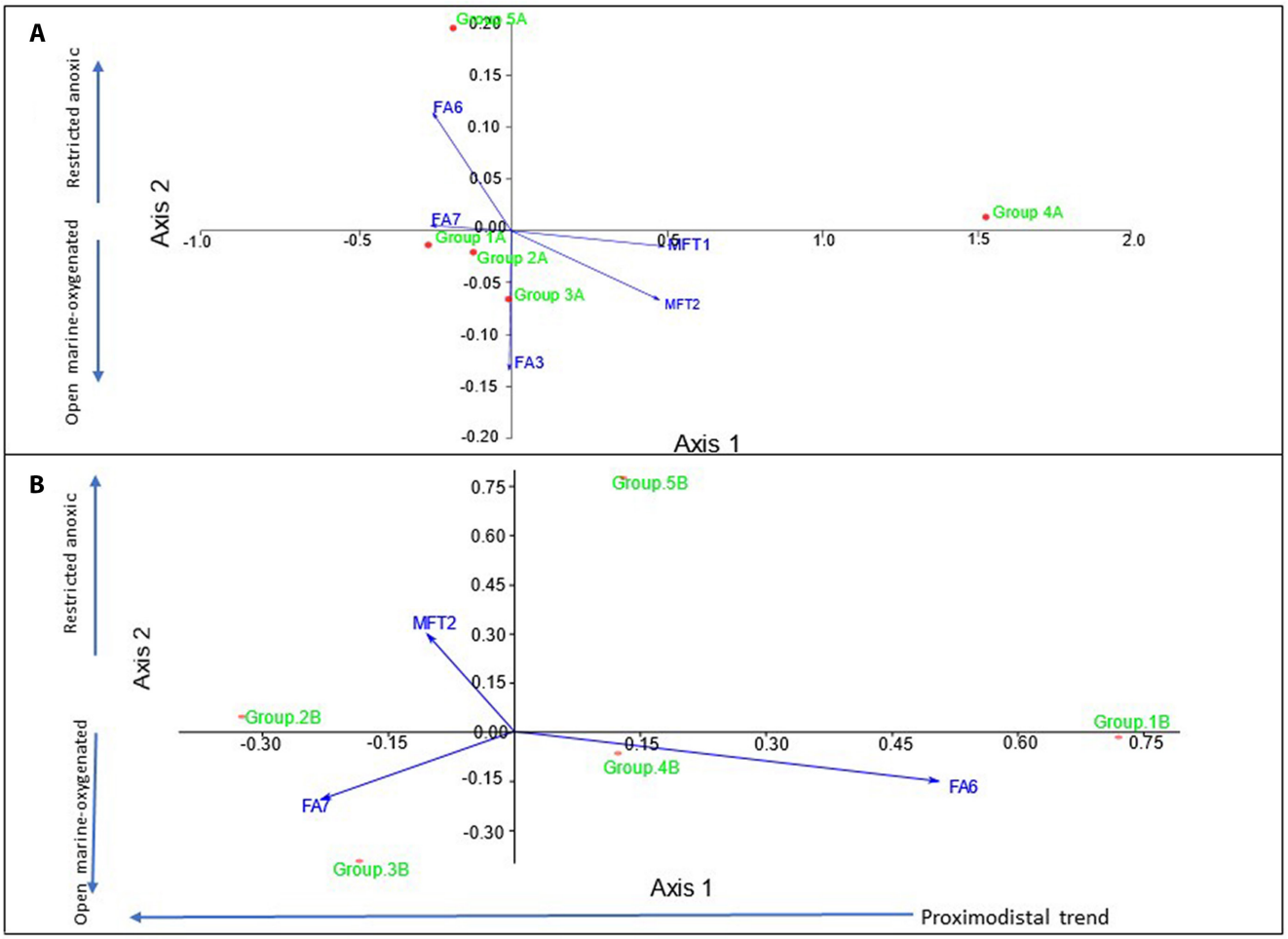

FIGURE 13 CCA plot showing the sedimentological variable and palaeoecological communities: (A) Yolde-Dukul-Jessu interval. (B) Sekule-Numanha-Lamja interval. For the Yolde-Dukul-Jessu interval axis one reflects proximal distal trend. The second axis reflects water circulation with open marine circulation at the lower and restricted circulation at the upper part. For the Sekule-Numanha-Lamja interval axis one reflects proximal distal trend. The second axis reflects water circulation.

microplankton groups 2B, 4B and 4A. The increase in the Cu: Zn (Figure 12) ratio is potentially related to stratified and restricted water microplankton groups 5A. Peridinioid microplankton groups 4A, 4B and 5B are highly related to lower Cu: Zn ratios whereas the decrease in Si:Al ratios is linked to the presence of peridinioid groups 3A and 3B. The results indicate that the geochemical values are correlated to compositional variability of the microplankton groups. In addition, $\delta^{13}C_{org}$ values of the shale samples range from −22.76 to −27.07‰ with a positive excursion within the Dukul Formation (Table 4, Figure 10).

5 | INTERPRETATIONS

Lithofacies analyses indicate that Cretaceous strata from the Upper Benue Trough were deposited under a range of environmental settings (Table 1). The Yolde Formation, which represents the onset of marine influence in the Upper Benue Trough, is characterised by temporal change in depositional environments. The lower part of the formation is characterised by facies associations FA1 (outer estuarine channels or tidal bar), FA2 (inner estuarine channels), FA3 (Middle estuarine), and FA4 (tidally influenced fluvial channels) (Table 2). These facies associations suggest that the lower part of the Yolde Formation was deposited in estuarine environments. The estuarine sequences are succeeded by facies associations FA5 (shoreface), FA6 (offshore transition) and FA7 (outer shelf) (Table 2) that are characterised by fining upward sequences. The planar and trough cross-bedded sandstones grade into hummocky cross-stratified sandstones, to wave ripple sandstones, and are finally capped by shale, suggesting they are a transgressive shelf deposit. The change from estuarine to shelf environments could be due to transgression that led to an abrupt change or shift in depositional conditions. The upper part of the Yolde Formation is characterised by a coarsening upwards that grades from facies association FA6 (offshore transition) to FA5 (shoreface) (Table 2) that

TABLE 4 Stable isotope data of $\delta^{13}C_{org}$ values obtained from bulk analysis of shale samples of the Upper Benue Trough.

Sample	$\delta^{13}C$ VPDB	Sample	$\delta^{13}C$ VPDB
BEJ9	−26.1	GWS25	−25.5
KUJ2	−26.8	GWS19	−25.5
LAJ1	−25.2	GWS13	−25.9
LAJ5	−25.9	CYNS9	−26.1
LAJ7	−26.1	GW5	−25.7
S14	−25.4	GWS2	−25.0
S12	−25.4	GWS1	−25.8
S9	−26.7	CH4	−26.5
S7	−27.1	CH2	−26.0
S2	−26.4	CHY29	−26.0
S2A	−26.1	CHY19	−24.9
DUOL1	−24.4	CHY15	−26.8
DKD9	−23.5	CHY7	−26.3
DKD6	−22.8	CHY3	−24.8
DKD5	−22.9	CHY1	−26.1
DKD	−23.2	BEJ1A	−24.7
DKY	−24.6	BEJ2A	−24.6
BY6	−24.4	BEJ3A	−25.9
BY4	−24.4	BEJ5	−25.8
BY3	−24.6	BEJ7	−25.9
		BEJ8	−25.2

suggest regressive deposits. This generally suggests that the Yolde Formation represents a short cycle of a transgressive-regressive sequence. The preservation of microplankton in the Yolde Formation from the estuarine, and shelf, facies successions are very poor, only a few spores, pollen and algae were recovered. The facies associations for the Yolde Formation are consistent with fluvial-estuarine, transgressive and regressive shelf depositional settings. This suggests a tripartite division of depositional environments which differs from earlier findings (Zaborski et al., 1997; Sarki Yandoka et al., 2015) that suggested shelf depositional environments.

The Dukul Formation, which overlies the Yolde Formation, is characterised by shale and clay intercalated with limestone beds. The limestones range between 20 to 35 cm thick. The formation is characterised by facies associations MFT1 and MFT2 (lagoonal). Macrofossils such as ammonites, gastropods and bivalves were recorded from the limestone beds. The shale shows good preservation of the microplankton. The microfossil recorded from this formation comprise peridinioids, gonyaulacoids, freshwater algae, spores and pollen. Petrography of the limestones shows that the beds include phosphatic grains. The abundance of these grains increases upward within the limestone beds and is linked with the occurrence of ammonites and an increase in gastropod abundance. Electron microscopy of the limestones shows that phosphate precipitated inside shells of ostracods, gastropods and bivalves (Figure 14). The Dukul Formation is overlain by coarsening upwards arenaceous strata of the Jessu Formation. The Jessu Formation consists of an arenaceous basal unit and thick shale interbedded with mudstone or fine-grained sandstone. The sandy basal unit is characterised by poor microfossil preservation, and the facies succession is interpreted as shoreface-offshore marine strata. For the thick intercalated part, the mudstones are bioturbated with *Thalassinoides*, and microfossil preservation is good, leading to high frequencies of microplankton recovery. The facies succession for the intercalated shale/clay and mudstone is interpreted as inner to outer shelf environment.

The Sekule Formation conformably overlies the Jessu Formation. The formation is characterised by shale and limestone beds that range in thickness between 10 to 45 cm. The Sekule Formation comprises facies associations MFT1 (lagoon) and MFT2 (partially restricted lagoon), similar to the Dukul Formation. The palynological data showed good preservation of freshwater algae, peridinioid dinocysts, gonyaulacoid dinocysts, spores and pollen. The petrographic data shows that the limestone contained whole-body bryozoans, bivalves and ostracods, which suggests deposition in lagoonal conditions. The samples indicate a periodic change in microplankton assemblage composition. This variation may be related to changes in depositional conditions.

The Numanha Formation comprises dominantly shale and clay with thin beds of mudstone associated with concretions. The rock of the Numanha Formation is attributed to facies association FA7 (outer shelf), including grey to dark grey shales with good microplankton preservation. Microplankton floras are dominated by peridinioid and gonyaulacoid dinocysts, while freshwater algae, spores and pollen frequencies are lower than those recorded from the Dukul, Jessu and Sekule formations. The dominance of shale lithology and associated marine microplankton of this formation indicates deposition in an outer shelf marine environment.

The Lamja Formation is the youngest stratigraphic unit in the Yola Sub-basin. It comprises fine-grained sandstones, shales and clays that formed in upper to middle shoreface (FA5) and offshore transition (FA6) facies associations. Fossiliferous limestone beds and a thin coal seam cap the coarsening upwards trend of these beds. These facies associations suggest deposition in lagoons and marshy environments. Both marine and terrestrial palynomorphs have been recorded from this formation. Freshwater algae dominate in facies association FA5, indicating a strong freshwater influence. Increased frequencies of peridinioid dinocysts, microforaminiferal test linings and gonyaulacoid *Oligosphaeridium* spp. dinocysts have been recorded from the offshore transition facies association.

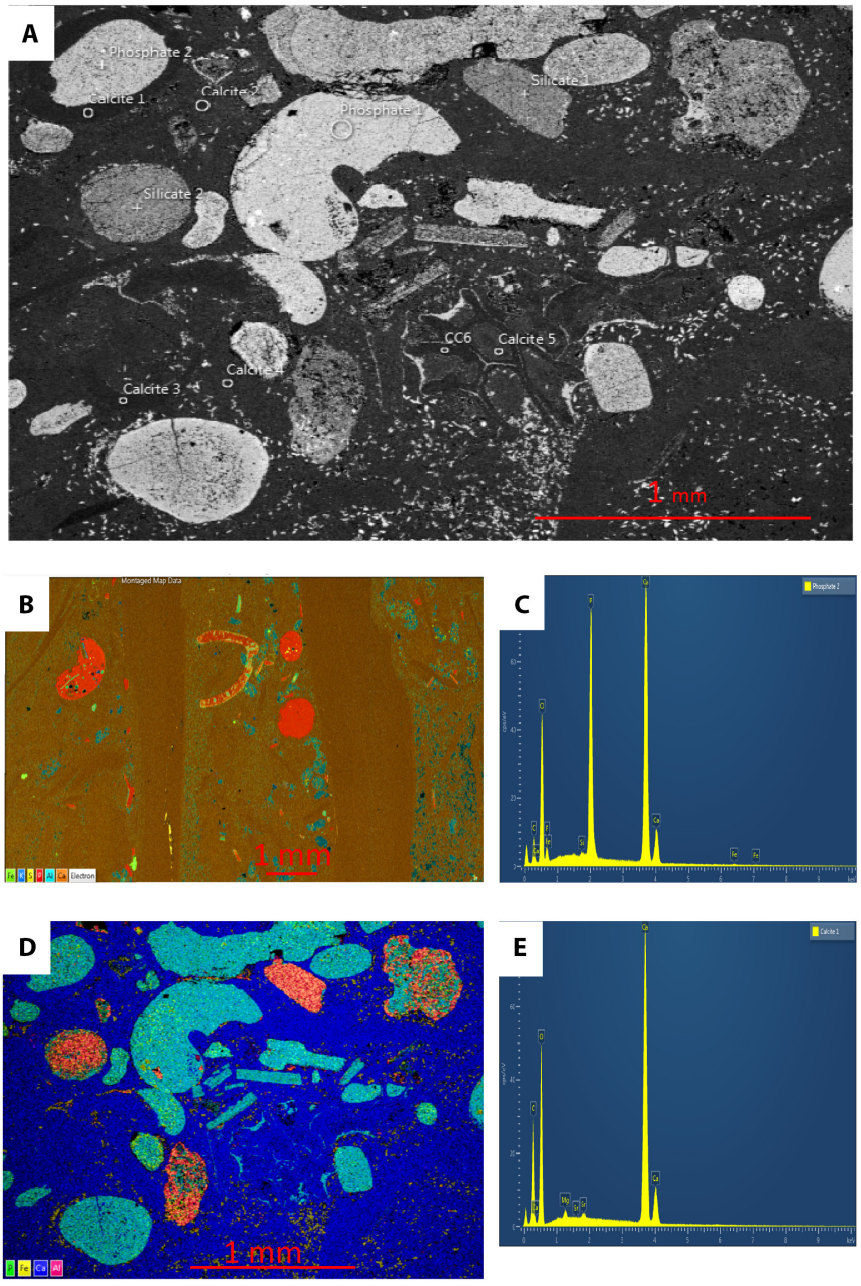

FIGURE 14 (A) SEM image shows phosphate, calcites and silicate grains. (B) and (D) ESD map shows phosphate and pyrite infilling bivalve and gastropod grains. (C) and (E) Chemistry of the grains in image A. Scale of each photograph is indicated by scale bar.

As indicated on Figure 4 the major variations between the Dukul, Jessu, Sekule and Numanha formations were a result of changes in siliciclastic input, which were high during the deposition of the Jessu and Numanha formations (Figure 4). Decrease in siliciclastic input favoured carbonate precipitation during deposition of the Dukul and Sekule formations. Therefore, the strata were divided into siliciclastic shelf and carbonate lagoon deposits.

5.1 | Microplankton Group Ecology

The DCA plots show distinctive compositional microplankton groups that reflect the ecological conditions that controlled their distribution (Figure 11). These microplankton groups were classified by their different ecological conditions, and the mechanisms that control their distribution are discussed below. Group compositions seem to reflect the nature of the water masses and proximal-distal trends (Appendix 1).

Freshwater group (1B) from the Sekule-Numanha-Lamja interval consists of *Pediastrum* sp. and *Scenedesmus* sp. (Figure 3B). Occurrence of these freshwater Chlorophyceae likely indicates input of fresh or brackish water into the basin (Batten, 1996). The maximum frequencies of the freshwater group occur in the arenaceous Lamja Formation (Figure 11), whereas microplankton groups were rare to absent in those strata. Correlation of the freshwater group with the offshore transition lithofacies (Table 2, FA6), and with a proxy for increased abundance

of heavy minerals (using the Zr:Al ratio as proxy for heavy minerals), is consistent with increased coarse siliciclastic input (Figures 12B and 13B) linked to high turbidity within the coastal zone (Muller, 1959; Batten, 1996).

The DCA of the two separate (Yolde-Dukul-Jessu and Sekule-Numanha-Lamja) stratigraphic intervals demonstrated that the taxonomic composition of the inner to outer neritic groups (Groups 1A, 2A and 2B) are comparable. Recovered from grey to dark grey shales, gonyaulacoid dinocysts and microforaminiferal test linings (oxygenated water) dominate the inner to outer neritic groups (Table 3). Foraminifera assemblages of the Upper Benue Trough are predominantly benthic and were mostly associated with oxygenated water masses (Petters, 1978, 1979), Thus, their abundance here may reflect deep and oxygenated conditions during deposition. Inner to outer neritic dinocyst groups show weak correlation with proxies of reducing conditions (using the Zn:Cu ratio as a proxy of reducing conditions), thereby suggesting oxygenated conditions prevailed in those settings (Figure 12). These microplankton groups are correlated with facies associations MFT2 (partially restricted lagoonal), FA3 and FA7 (i.e. middle estuarine to outer shelf environments; Figure 13); also, their correlation with arenaceous components (Figure 12) suggests high turbidity depositional conditions. They were probably deposited in an oxygenated, estuarine–outer shelf marine environment.

A transition from gouyaulacoid to peridinioid dinocyst-dominated microplankton groups (Figure 3A,B and Table 3) is seen in cosmopolitan groups (3A and 3B). These groups were related to shallow to outer shelf environments (facies associations FA6 and FA7 and MFT2; Figure 13) and show a weak correlation with proxies of an increase in the heavy mineral component (Figure 12). Cosmopolitan groups (3A and 3B) also have an overlap with autotrophic microplankton groups (oxygenated neritic Groups 2A and 2B), and also with heterotrophic groups (peridinioid-stratified groups 4A and 4B) (Figure 3). This implies that cosmopolitan groups (3A and 3B) were probably influenced by taphonomy and not true ecological groups or maybe tolerance to different water mass settings.

Peridinioid-dominated groups (peridinioid-stratified groups 4A and 4B) include *Subtilisphaera* spp., *Deflandrea* spp. and *Alterbidinium* spp. These groups 4A and 4B were recovered from dark grey shales and they have a weak correlation with freshwater algae (Figures 3B and 11). Low frequencies of microforaminiferal test linings are associated with peridinioid-stratified groups (4A and 4B), and could be associated with oxygen deficiency at the sediment–water interface (Petters, 1981). Peridinioid-stratified groups are correlated with high Si:Al ratios (low clay?) (Figure 12) and are consistent with a water mass that was stratified. From these correlations, it is suggested that these peridinioid-stratified groups (4A and 4B) were linked to offshore transition and lagoonal environments (Figure 13), with poorly circulated, stratified water masses.

Peridinioid-restricted groups (5A and 5B) are primarily dominated by *Eurydinium* spp. and other peridinioid dinocysts (Table 3). They were recovered from dark grey shales with low frequencies of algae and microforaminiferal test linings. The, peridinioid-restricted groups (5A and 5B) are associated with dwarf bivalves which suggests linkage to a hypersaline restricted environment (Flügel, 2010). In contrast to other groups, the peridinioid-restricted group (5A) shows positive correlation with high Cu:Zn ratios (Figure 12) suggesting reducing conditions. Furthermore, the CCA-sedimentological plots for these groups indicate that they are related to lithofacies associations of offshore transition and and lagoonal environments (FA6 and MFT1) (Figure 13). From these correlations, it is suggested that these peridinioid-restricted groups (5A and 5B) were linked to restricted, stratified water masses.

5.2 | Cenomanian–Santonian Strata

Combined sedimentological and palynological approaches were employed to delineate the relative sea-level changes within the Cenomanian –Santonian strata of the Yola Sub-basin. First the sedimentogical and palynological data were used independently to delineate the relative sea-level changes and the two methods were later combined for robust identification of the depositional sequences. The sedimentological data of the Yola Sub-basin indicates that the Cenomanian–Santonian strata were deposited in estuarine to outer shelf environments with dominant shelf strata. The Yola Sub-basin is one of the epicontinental seas primarily characterised by a ramp setting; therefore, coarser sediments were deposited during the fall in sea level in the distal shelf setting. Because of this, for the sedimentological data, an abrupt increase in siliciclastic grain size up section suggests an influx of sediment, potentially related to relative sea-level fall. Therefore, a subtle or major change in grain size from the lithostratigraphical section (minor for the outer shelf and major for shoreface and offshore transitional environments) was used to define depositional sequence boundaries (SB) and an increase in clay for the maximum flooding surfaces (MFS) (Figures 10 and 11). Based on these criteria, the Lowstand System Tract (LST) is defined by an increase in grain size. An increase in fine argillaceous material defines the transgressive system tract (TST), whereas a decrease in argillaceous material above the MFS defines the Highstand System Tract (HST).

For the palynological data set, a combined microplankton assemblage, microplankton Shannon and dominance index approach was employed to delineate depositional sequences of the Cenomanian–Santonian strata of the Yola Sub-basin,

independently of the sedimentological sequences defined above, to test this approach. The SB is here defined by low microplankton Shannon diversity and high dominance diversities and dominance of Chlorophyceae microplankton. In contrast, high Shannon diversity and low dominance index define the MFS (Figures 10 and 11). The LST is characterised by low Shannon diversity and high dominance index, high freshwater algae assemblages and low gonyaulacoid and peridinioids dinocysts groups. The TST is characterised by high gounyalacoid and low peridinioid dinocyst groups with higher Shannon diversity and low dominance index (Figures 10 and 11). A high frequency of peridinoid groups, a low frequency of the gounyalacoid dinocyst groups, a decrease in Shannon diversity and an increase in dominance index characterised the HST (Figures 10 and 11).

For robust depositional sequence analysis, the sedimentological and the palynological approaches were then combined. The two methods compared well because all the depositional sequences identified have marched. However, the palynological method provides a clearer way of identifying the MFS. The palynological approach helps to delineate a depositional sequence in the distal part where there is no sedimentological evidence to deduce the relative sea-level changes. For example, the base of the depositional sequence VII does not show sedimentological evidence, but a fourth-order sequence is identified from the palynological data.

In general, a grain size increase combined with a decrease in Shannon diversity is taken here as a sequence boundary. For example, a decrease in Shannon diversity index at 71 m depth in the Yolde-Dukul-Jessu interval (Figure 10) occurs in sedimentary rocks that exhibit hummocky cross-stratification, plus herringbone, trough and planar crossbedding (FA5-shoreface). The SB at 21 m depth of the Sekule-Numanha-Lamja interval (Figure 11) exhibits sedimentary rocks characterised by coquina limestone beds and sandstone (MFT1-carbonate lagoon), and at 176 m depth (Figure 11) the sediment is characterised by 8 cm small scale crossbedding and ripple lamination (FA5-Shoreface). Therefore, where the sedimentological data are not so clear (including correlative conformities), the decrease in Shannon diversity can still be used to help tentatively define sequence boundaries. With the laboratory-determined data (Shannon diversity) presented here it would be possible for future studies to re-visit the field sites and look for subtle changes in the sedimentology around the proposed SBs.

For MFSs, microplankton diversity and abundance gradually rise as the abundance of argillaceous material increases. This could be explained by decreased turbidity and increased salinity associated with relative sea-level rise. Following this model, MFS can be identified where there is a combination of maximum microplankton diversity (≥2.5), high abundance of argillaceous material, and low dominance index (≤0.3) value.

For LSTs, an increase in grain size of siliciclastic deposits is interpreted as a shelf wedge sandstone LST deposit formed during the fall in relative sea level. The LSTs are poorly developed within some of the sequences identified in the Yola Sub-basin. However, where the LST is well preserved it is associated with low microplankton diversity and dinocyst frequency, and high frequencies of freshwater algae (group 1B). A LST is formed during the falling stage of sea level, which is characterised by high fluvial input, decrease in depth, and high turbidity, resulting in highly stressed ecosystems. The low diversity (≤2.0) and low frequency of marine microplankton may be due to high turbidity and low salinity associated with LST (Figures 9 and 10). The increase in abundance of freshwater algae in the LST is likely caused by *Pediastrum* and *Scenedesmus* being adapted to freshwater and low salinity conditions (Tappan, 1980).

The TST, is characterised by an increase in microplankton diversity, abundance of inner to outer neritic microplankton groups and an increase in argillaceous material above the LST. Increased microplankton abundance and diversity, including oxygenated inner to outer neritic microplankton groups (Groups 1A, 2A and 2B), indicate open marine circulation during the transgressive systems tract (TST) (Figures 10 and 11). The abundance of freshwater groups decreased as ocean depth increased during TSTs. Being further from the shoreline at these times, proportionally fewer marginal freshwater sediments were transported this far offshore.

The HSTs are marked by a gradual decline in the microplankton diversity index and a decrease in microforaminiferal test linings, and by low frequency of algae that suggests basin isolation, and arguably a rise in the oxygen minimum zone. Additionally, peridinioid assemblages of stratified to restricted water masses (Groups 4A, 5A, 4B and 5B) became dominant; this is taken as indicative of HST.

Using these criteria, a series of depositional sequences have been here identified within the Yola Sub-basin (Table A1). This allows the delineation of seven third-order sequences and one fourth-order sequence (Figures 10 and 11) from the strata of the Yola Sub-basin. The high-resolution sampling employed permits delineation of parasequences associated with the sequences. Parasequences are shorter wavelength transgressive-regressive units bounded by maximum regressive surfaces and their correlative surfaces (sensu Embry, 2009). The palynological patterns observed in a parasequence are characterised by an increase in diversity, and by occurrence of restricted to stratified water peridinioid dinocyst assemblages at the bounding surface. Based on these criteria, 20 parasequences were defined from Cenomanian–Santonian rocks of the Yola Sub-basin (Figures 10 and 11).

6 | DISCUSSION

The distribution of peridinioid dinocysts in the Yola Subbasin is best interpreted as related to nutrient influx and oxygen depleted water masses. Similar trends were observed from Cenomanian–Turonian strata of "black shale" sequences of northern Europe (Marshall & Batten, 1988) and the Western Interior Seaway of North America, and equatorial Atlantic basins (Eldrett et al., 2017). High frequencies of peridinioid dinocysts in this study can be related to low microforaminiferal test lining abundances during highstands. It was found that low recovery of the microforaminifera assemblages within the rocks of the Benue Trough were linked to anoxic condition (Petters, 1978, 1979). Therefore, the low microforaminiferal test linings abundance was caused by low oxygenation due to water stratification. Similar findings were reported by Peyrot et al. (2012) and Eldrett et al. (2017), who related such a trend to suboxic–anoxic marine conditions. Modern peridinioids have been linked to environments with fluctuating salinity and availability of nutrients (Wall et al., 1977). The association of peridinioid groups with apparent influx of heavy minerals suggests an influence of turbidity, or perhaps a fluvial plume, which was probably the source of nutrients. This could also have caused pycnocline separation between less saline surface and high saline deeper water. The water stratification would have restricted vertical mixing and led to oxygen depletion in the bottom layer, thereby leading to anoxic conditions. This is supported by dominance of peridinioid assemblages at the positive excursion of $\delta^{13}C_{org}$ (Figure 10) that would be consistent with an OAE. This likely OAE is recorded in strata deposited during the Cenomanian stage based on palynozonation presented by Usman et al. (2021), such that it is likely to be OAE 2. Microplankton assemblages from the Cenomanian–Turonian of Spain indicated temporal variations between peridinioid and gonyaulacoid dinocysts (Peyrot et al., 2012). However, Peyrot et al. (2012) indicated no anoxic conditions related to their recorded data, and instead the peridinioid dinocysts were linked to a cold climate but, this study indicates that peridinioid dinocysts were linked to warm and stratified water. Carvalho et al. (2016) recorded *Subtilispheara* assemblages from Aptian–Albian dark grey shales of the Sergipe Basin, linked to nutrient availability associated with a fluvial plume.

Studies of recent dinoflagellate cyst assemblages have indicated that gonyaulacoid dinocysts are associated with estuarine and open marine environments (Wall et al., 1977). Similarly, gonyualacoid dinocysts recorded in this study (Table 3) indicate similar ecology with the extant gonyaulacoid dinocysts. High abundance of the gonyaulacoid dinocyst groups are associated with high frequencies of microforaminiferal test linings, in a record similar to that recorded by Peyrot et al. (2012) and Eldrett et al. (2017). The high frequency of the microforaminiferal test linings has been interpreted as an indication of open marine depositional conditions (Batten, 1982). The foraminifera require well oxygenated waters to thrive, which could be best achieved during episodes of basin mixing (Petters, 1978, 1979). The abundance of these microforaminiferal test linings, and associated dinocysts produced by autotrophic dinoflagellates in this study, indicates deposition in oxygenated open marine environments related to rising relative sea levels.

The combined sedimentological and statistical palynological approach presented here can be used to help delineate depositional sequences, and to refine stratigraphic correlations for three geographical units of the Benue Trough and other coeval basins. The demonstrable value of this approach is that it removes inherent problems associated with the widely used terrestrial:marine ratio (Prauss, 1993, 2001; Helenes & Somoza 1999) that does not allow for the impact of salinity layering, sediment plumes, basin structure or varying hydrodynamic properties in microspore morphotypes. This concept could be applied to other basins worldwide to help delineate their depositional sequences. The concept could also find useful applications in shallow and deeper marine strata where the conventional sedimentological method is highly challenging, and this has the potential to enhance our understanding of depositional packages in these settings.

6.1 | Cenomanian–Turonian anoxic event

Results from stable isotopic analysis of shale samples from the Upper Benue Trough reveal a positive isotope excursion within the Dukul Formation. The formation was dated Cenomanian using terrestrial palynomorphs (Usman et al., 2021). To determine Cenomanian–Turonian anoxic events samples were collected from strata deposited during that time (Yolde, Dukul, Jessu and Sekule). The Dukul Formation which records this excursion consists of limestone beds including gastropods, ammonites, bivalves, ostracodes, calcispheres and miliolid foraminifera. Below the isotopic excursion are rocks exhibiting relatively large bivalves, whereas sediments deposited during the isotopic excursion were characterised by smaller bivalves and phosphatic peloidal grains. The lagoonal sediments deposited during the excursion were also associated with increased microfossil and macrofossil abundance.

Petrography and geochemistry suggest that phosphates precipitated inside the shells of ostracods, gastropods and bivalves (Figure 14) were syn-depositional to early burial in timing. The phosphates are commonly associated with pyrite and ferroan calcite cements (Figures 9 and 14)

indicating low oxygen conditions, consistent with being in a high-productivity restricted environment where nutrients were supplied from terrestrial influxes. Such influxes would also provide some calcium for calcium phosphate, but the poor oxygenation would mean that the phosphate was not immediately utilised by living organisms, low alkalinity or likely inhibited calcite growth (Ruttenberg, 2003). Although the effects of burial alteration in producing the ferroan calcite cements cannot be fully ruled out, it seems likely that since the phosphates were syn-depositional then the matrix calcite was likely to be ferroan at the time of deposition.

The Dukul Formation represents the major onset of marine incursion into the Yola Sub-basin and the carbon excursion formed at the basal part of the formation. The underlying Yolde Formation is characterised by poor fossil preservation. Only low frequencies of algae, spores and pollen were recorded. High abundance of marine microplankton was only recorded from the Dukul Formation, coinciding with the major carbon excursion. Peridinioid dinocysts such as *Subtilispheara* spp. and *Palaeohystrichophora infusorioides* were the major microplankton recorded from this interval and gonyaulacoid and freshwater algae were also present. Land-derived Terrestrial palynomorphs such as pteridophytes, tricolpate pollen, *Classopollis Steevesipollenites*, *Elaterocolpites castelaini* and *Afropollis jardinus* are common. During this carbon excusion, the frequency of benthic microforaminiferal test linings was generally low in contrast to high frequencies of peridinioid dinocysts. The high frequency of peridinioid Groups 4A and 5A that are associated with enhanced Cu:Zn ratios is interpreted as deposition under anoxia or euxinia. The small (dwarf?) bivalves and low frequency of microforaminiferal tests linings in the Dukul Formation reflect deposition under stressed environmental conditions. Based on molecular geochemistry and microfacies studies, the formation was interpreted as deposition under suboxic/dyoxic to anoxic conditions by Ayuba et al. (2020) and Sarki Yandoka (2021). Therefore, these results suggest that in the Benue Trough OAE 2 was related to oxygen depleted stratified water. The identification of OAE 2 in the Benue Trough provides impetus for correlation of the strata from this basin with those of other contiguous basins.

7 | CONCLUSIONS

The sedimentological data indicate that Cenomanian–Santonian strata of the Yola Sub-basin of the Benue Trough were deposited in estuarine, lagoon and shelf environments. The Yolde Formation which overlies the Bima Formation that was deposited in continental environments (Carter et al., 1963), marked the first marine incursion into the Upper Benue Trough. The Yolde Formation was deposited in estuarine and shelf environments. These sediments also mark the oldest marine transgression into the Upper Benue Trough. This contrasts with the interpretation of earlier authors (Zaborski et al., 1997; Sarki Yandoka et al., 2015) who interpreted them as regressive shoreface deposits. Furthermore, the depositional environments of Dukul and Sekule suggest lagoon whereas Jessu, Numanha and Lamja formations indicate deposition in shelf settings.

The distribution of microplankton groups was recorded in Cenomanian–Santonian strata of the Yola Sub-basin. A statistical approach to interpreting such data was shown to be effective in delineation of proximal distal transects, understanding of ancient water masses, and correlation of depositional sequences.

A sequence stratigraphical framework for Cenomanian–Santonian strata of the Benue Trough has been derived from microplankton ecology and lithofacies variation. In all sequences, the SBs are related to an increase in grain size and low microplankton diversity, whereas the MFS is characterised by a maximum in microplankton diversity. The LSTs are related to high siliciclastic input and the increased Chlorophyceae microplankton group. The TSTs are mostly associated with oxygenated neritic gonyaulacoid dinocyst groups (1A, 2A and 2B) and increases in diversity, whereas peridinioid stratified to restricted water mass dinocyst groups (4A, 5A, 4B and 5B) dominate the HST and are associated with decreasing diversity. The increase in diversity from sequence boundaries to maximum flooding surfaces is interpreted as being related to shelf expansion due to flooding during transgression. Using a combination of traditional sedimentology and interpretation of microplankton data, seven third order, one fourth order and 20 parasequences were delineated from the strata of the basin.

This study has for the first time reported a carbon isotope excursion in strata from the Benue Trough. This carbon isotope excursion represents the first record of the Cenomanian–Turonian global anoxic event in the Trans-Sahara Seaway.

ACKNOWLEDGEMENTS

M.B. Usman thanks the Petroleum Technology Development Fund (PTDF) for funding this research at the University of Aberdeen. The editor and reviewer are also thanked for their corrections which improved the manuscript. We also acknowledge Stephen Ingram, Adamu Kimayim Gaduwang and Solomon Abafras for their contributions.

DATA AVAILABILITY STATEMENT

All studied and illustrated specimens are achieved in the collections of the Department of Geology and Geophysics at the University of Aberdeen under Musa Usman PhD using sample numbers as reported adjacent to log in Figures 4, 10 and 11.

ORCID

Musa B. Usman https://orcid.org/0000-0001-9989-6115

REFERENCES

Allison, P.A. & Wells, M.R. (2006) Circulation in large ancient epicontinental seas: What was different and why? *Palaios*, 21, 513–515.

Arning, E.T., Birgel, D., Brunner, B. & Peckmann, J. (2009) Bacterial formation of phosphatic laminites off Peru. *Geobiology*, 7(3), 295–307.

Ayuba, M.K.S., Yandoka, B.M., Muhammed, M., Samaila, N.K., Maigari, A.S. & Bata, T. (2020) Molecular geochemistry of Cretaceous Dukul Formation, Yola Sub-basin, Northern Benue Trough, Nigeria: Origin, paleoredox condition, and thermal maturity. *Science Forum (Journal of Pure and Applied Sciences)*, 20, 81–89.

Batten, D.J. (1982) Palynofacies, palaeoenvironments and petroleum. *Journal of Micropalaeontology*, 1, 107–114.

Batten, D.J. (1996) Colonial Chlorococcales. In: *Palynology: Principles and Applications*, Vol. 1, Dallas, TX: American Association of Stratigraphic Palynologists Foundation, pp. 191–203.

Benkhelil, J., Dainelli, P., Ponsard, J.F., Popoff, M. & Saugy, L. (1988) The Benue trough: Wrench-fault related basin on the border of the equatorial Atlantic. *Developments in Geotectonics*, 22, 787-819

Bloch, J. (1998) Shale diagenesis: a currently muddied view. In: Schieber, J., Zimmerle, W. & Sethi, P.S. (Eds.) *Shales and Mudstones, Volume I. Basin studies, Sedimentology and Paleotology*. Stuttgart: E. Schweizerbart'sche Verlagsbuchhandlung (Nägele u. Obermiller). Stuttgart, pp. 96–106.

Boyd, R., Dalrymple, R.W. & Zaitlin, B.A. (1992) Classification of clastic coastal depositional environments. *Sedimentary Geology*, 80, 139–150.

Brinkhuis, H. (1994) Late Eocene to Early Oligocene dinoflagellate cysts from the Priabonian type-area (Northeast Italy): biostratigraphy and paleoenvironmental interpretation. *Palaeogeography, Palaeoclimatology, Palaeoecology*, 107, 121–163.

Buzas, M.A. (1979) The measurement of species diversity. In: Lipps, J.H., Berger, W.H., Buzas, M.A., Douglas, R.G. & Ross, C.A. (Eds.) *Foraminiferal Ecology and Paleoecology, Short Course Notes 6: SEPM*. Tulsa, OK: Society for Sedimentary Geology, pp. 3–10.

Carter, J.D., Barber, W., Talt, E.A. & Jones, J.P. (1963) The geology of parts of Adamawa, Bauchi and Bomu provinces in Northeastern Nigeria. *Bulletin Geological Survey of Nigeria*, 30, 1–109.

Carvalho, M.D.A., Bengtson, P. & Lana, C.C. (2016) Late Aptian (Cretaceous) paleoceanography of the South Atlantic Ocean inferred from dinocyst communities of the Sergipe Basin, Brazil. *Paleoceanography*, 31, 2–26.

Clifton, H.E. (1982) Estuarine deposits. In: *Sandstone Depositional Environments*, Tulsa, Oklahoma: American Assocition of Petroleum Geologists, Vol. 31, pp. 179–189.

Dale, B. (1996) Dinoflagellate cyst ecology: Modeling and geological applications. In: *Palynology: Principles and Applications*, Vol. 3. Dallas, TX: American Association of Stratigraphic Palynologists Foundation, pp. 1249–1275.

Dalrymple, R.W., Zaitlin, B.A. & Boyd, R. (1992) Estuarine facies models: conceptual basis and stratigraphic implications. *Journal of Sedimentary Petrology*, 62, 1130–1146.

Dalrymple, R.W. & Choi, K. (2007) Morphologic and facies trends through the fluvial–marine transition in tide-dominated depositional systems: a schematic framework for environmental and sequence-stratigraphic interpretation. *Earth-Science Reviews*, 81(3–4), 135–174.

Dalrymple, R.W. (2010) Tidal depositional systems. In: James, N.P. & Dalrymple, R.W. (Eds.) *Facies models 4*. St John's: Geological Association of Canada, pp. 201–231.

Desjardins, P.R., Buatois, L.A. & Mangano, M.G. (2012) Tidal flats and subtidal sand bodies. In: *Developments in Sedimentology*, Vol. 64. Amsterdam: Elsevier, pp. 529–561.

Dott, R.H., Jr. & Bourgeois, J. (1982) Hummocky stratification: significance of its variable bedding sequences. *Geological Society of America Bulletin*, 93, 663–680.

Dumas, S. & Arnott, R.W.C. (2006) Origin of hummocky and swaley cross-stratification – the controlling influence of unidirectional current strength and aggradation rate. *Geology*, 34, 1073–1076.

Dunham, R.J. (1962) Classification of carbonate rocks according to depositional texture. In: Ham, W.E. (Ed.) *Classification of Carbonate Rocks American Association of Petroleum Geologists Memoirs*, Tulsa, Oklahoma: American Association of Petroleum Geologists, Vol. 1, pp. 108–121.

Eldrett, J.S., Dodsworth, P., Bergman, S.C., Wright, M. & Minisini, D. (2017) Water-mass evolution in the Cretaceous Western Interior Seaway of North America and equatorial Atlantic. *Climate of the Past*, 13, 855–878.

Embry, A.F. (2009) Practical sequence stratigraphy XII: the units of sequence stratigraphy: part 4 Parasequences. *Canadian Society of Petroleum Geologists, The Reservoir*, 36, 55–58.

Flügel, E. (2010) *Microfacies of carbonate rocks: Analysis, interpretation and application*. Berlin: Springer, p. 271.

Folk, R.L. (1959) Practical petrographic classification of limestones. *Bulletin of American Association of Petroleum Geologists*, 43, 1–38.

Garzon, S., Warny, S. & Bart, P.J. (2012) A palynological and sequence-stratigraphic study of Santonian-Maastrichtian strata from the Upper Magdalena Valley basin in central Colombia. *Palynology*, 36, 112–133.

Genik, G.J. (1993) Petroleum geology of Cretaceous-Tertiary rift basins in Niger, Chad, and Central African Republic. *American Association of Petroleum Geologists Bulletin*, 77, 1405–1434.

Guiraud, M. (1990) Tectono-sedimentary framework of the early Cretaceous continental Bima formation (upper Benue Trough, NE Nigeria). *Journal of African Earth Sciences*, 10, 341–353.

Hallberg, R.O. (1976) A geochemical method for investigation of paleoredox conditions in sediments. Ambio Special Report 4, 138–147.

Hammer, R., Harper, D.A.T. & Ryan, P.D. (2016) PAST: Paleontological statistics software package for education and data analysis. *Palaeontologia Electronica*, 4, 910.

Haq, B.U., Hardenbol, J. & Vail, P.R. (1987) Chronology of fluctuating sea levels since the Triassic. *Science*, 235(4793), 1156–1167.

Haq, B.U., Hardenbol, J. & Vail, P.R. (1988) Mesozoic and Cenozoic chronostratigraphy and cycles of sea-level change. In: *Sea-level changes: an integrated approach*, Tulsa: SEPM Special Publication, pp. 71–108.

Haq, B.U. (2014) Cretaceous eustasy revisited. *Global and Planetary Change*, 113, 44–58.

Harris, A.J. & Tocher, B.A. (2003) Palaeoenvironmental analysis of Late Cretaceous dinoflagellate cyst assemblages using high-resolution sample correlation from the Western Interior Basin, USA. *Marine Micropaleontology*, 48, 127–148.

Helenes, J. & Somoza, D. (1999) Palynology and sequence stratigraphy of the Cretaceous of eastern Venezuela. *Cretaceous Research*, 20, 447–463.

Hill, M.O. & Gauch, H.G. (1980) Detrended correspondence analysis: An improved ordination technique. *Vegetatio*, 42, 47–58.

Li, H. & Habib, D. (1996) Dinoflagellate stratigraphy and its response to sea level change in Cenomanian-Turonian sections of the western interior of the United States. *Palaios*, 11, 15–30.

Lowery, C.M., Leckie, R.M., Bryant, R., Elderbak, K., Parker, A., Polyak, D.E., Schmidt, M., Snoeyenbos-West, O. & Sterzinar, E. (2018) The Late Cretaceous Western Interior Seaway as a model for oxygenation change in epicontinental restricted basins. *Earth-Science Reviews*, 177, 545–564.

Marshall, K.L. & Batten, D.J. (1988) Dinoflagellate cyst associations in Cenomanian-Turonian "black shale" sequences of Northern Europe. *Review of Palaeobotany and Palynology*, 54, 85–103.

Miall, A.D. (1996) *The Geology of Fluvial Deposits, Sedimentary Facies, Basin Analysis, and Petroleum Geology*. New York: Springer, p. 582.

Muller, J. (1959) Palynology of recent Orinoco delta and shelf sediments. *Micropaleontology*, 5, 1–32.

Opeloye, S.A. (2012) Microfossils and Paleoenvironment of the Numanha Shale of the Upper Benue Trough, Northeastern Nigeria. *Journal of Mining and Geology*, 48(2), 167–175.

Palmer, M.W. (1993) Putting things in even better order: The advantages of Canonical Correspondence Analysis. *Ecology*, 74, 2215–2230.

Patten, B.C. (1962) Species diversity in net phytoplankton of Raritan Bay. *Journal of Marine Research*, 20, 57–75.

Petters, S.W. (1978) Stratigraphic evolution of the Benue Trough and its implications for the Upper Cretaceous paleogeography of West Africa. *Journal of Geology*, 86, 311–322.

Petters, S.W. (1979) Paralic arenaceous foraminifera from the Upper Cretaceous of the Benue Trough, Nigeria. *Acta Palaeontologica Polonica*, 24, 451–471.

Petters, S.W. (1981) Paleoenvironments of the Gulf of Guinea. Proc. 26th Int. Geol. Congr. Oceanol. Acta, 81–85.

Peyrot, D., Barroso-Barcenilla, F. & Feist-Burkhardt, S. (2012) Palaeoenvironmental controls on late Cenomanian-early Turonian dinoflagellate cyst assemblages from Condemios (Central Spain). *Review of Palaeobotany and Palynology*, 180, 25–40.

Pielou, E.C. (1969) *An Introduction to Mathematical Ecology*. New York: John Wiley, p. 286.

Plint, A.G., James, N.P. & Dalrymple, R.W. (2010) Wave-and storm-dominated shoreline and shallow-marine systems. *Facies Models*, 4, 167–201.

Powell, A.J., Lewis, J. & Dodge, J.D. (1992) *The palynological expressions of post-Palaeogene upwelling: A review*. In Sammerhayes, C.P.. Prell, W.L. & Emeis, K.C. (Eds.) Upwelling System: Evolution Since the Early Miocene, London: Geological Society, Special Publication, p. 64.

Powell, A.J., Brinkhuis, H. & Bujak, J.P. (1996) Upper Paleocene-Lower Eocene dinoflagellate cyst sequence biostratigraphy of southeast England. In: Knox, R.W.O.B., Dunay, R.E. (Eds.), *Correlation of the Early Paleogene in Northwest Europe Geological Society*, London: Special Publication, 101, pp. 145–185

Prauss, M. (1993) Sequence palynology - Evidence from Mesozoic sections and conceptual framework. *Neues Jahrbuch für Geologie und Paläontologie Abhandlungen*, 190, 143–163.

Prauss, M. (2001) Sea-level changes and organic-walled phytoplankton response in a Late Albian epicontinental setting, Lower Saxony basin, NW Germany. *Palaeogeography, Palaeoclimatology, Palaeoecology*, 174, 221–249.

Reynaud, J.Y. & Dalrymple, R.W. (2012) Shallow-marine tidal deposits. In: *Principles of Tidal Sedimentology*, Dordrecht: Springer, pp. 335–369.

Ruttenberg, K.C. (2003) The global phosphorus cycle. In: *Treatise on geochemistry*, Vol. 8, Pergamon: Oxford, p. 682.

Saker-Clark, M., Kemp, D.B. & Coe, A.L. (2019) Portable Xray fluorescence spectroscopy as a tool for cyclostratigraphy. *Geochemistry, Geophysics, Geosystems*, 20, 2531–2541.

Sarki Yandoka, B.M., Abubakar, M.B., Abdullah, W.H., Maigari, A.S., Hakimi, M.H., Adegoke, A.K., Shirputda, J.J. & Aliyu, A.H. (2015) Sedimentology, geochemistry and paleoenvironmental reconstruction of the Cretaceous Yolde formation from Yola Sub-basin, Northern Benue Trough, NE Nigeria. *Marine and Petroleum Geology*, 67, 663–677.

Sarki Yandoka, B.M. (2021) Microfacies Analysis of Cretaceous Sediments of Dukul Formation, Yola Sub-Basin, Northern Benue Trough, Nigeria: Paleo-Environmental Implications *FUDMA Journal of Sciences*, 5 No. 2, 310-319

Sarki Yandoka, B.M., Abdullah, W.H., Abubakar, M.B., Johnson, H., Adegoke, A.K., Arabi, A.S., Bata, T.P., Amir Hassan, M.H., Mustapha, K.A. & Usman, M.B. (2019) Shoreface facies model of Cretaceous Jessu Formation, Yola Sub-basin, Northern Benue Trough, northeast Nigeria: New insights from facies analysis and molecular geochemistry. *Journal of African Earth Sciences*, 152, 10–22.

Schlanger, S.O. & Jenkyns, H.C. (1976) Cretaceous Oceanic Anoxic Events: Causes and Consequences. *Geologie en Mijnbouw*, 55, 179–184.

Scotese, C.R. (2014) *Atlas of Late Cretaceous Maps. PALEOMAP Atlas for ArcGIS 2. The Cretaceous, Maps 16–22, Mollweide Projection*. Evanston, Illinois: PALEOMAP Project.

Simpson, E.H. (1949) Measurement of diversity. *Nature*, 163, 688.

Stukins, S., Jolley, D.W., McIlroy, D. & Hartley, A.J. (2013) Middle Jurassic vegetation dynamics from allochthonous palynological assemblages: An example from a marginal marine depositional setting; Lajas Formation, Neuquén Basin, Argentina. *Palaeogeography, Palaeoclimatology, Palaeoecology*, 392, 117–127.

Tappan, H. (1980) *The paleobiology of plant protists*. New York: Freeman, pp. 1–1028.

Ter Braak, C.J.F. (1986) Canonical correspondence analysis: a new eigenvector technique for multivariate direct gradient analysis. *Ecology*, 67, 1167–1179.

Usman, M.B., Brasier, A.T., Jolley, D.W., Abubakar, U. & Mukkafa, S. (2021) Did the Benue Trough connect the Gulf of Guinea with the Tethys Ocean in the Cenomanian? New evidence from the palynostratigraphy of the Yola Sub-basin. *Cretaceous Research*, 119, 1–16

Varban, B.L. & Guy Plint, A. (2008) Palaeoenvironments, palaeogeography, and physiography of a large, shallow, muddy ramp: Late Cenomanian-Turonian Kaskapau Formation, Western Canada foreland basin. *Sedimentology*, 55(1), 201–233.

Wall, D., Dale, B., Lohmann, G.P. & Smith, W.K. (1977) The environmental and climatic distribution of dinoflagellate cysts in modern marine sediments from regions in the North and South Atlantic Oceans and adjacent seas. *Marine Micropaleontology*, 2, 121–200.

Watkins, D.K. (1989) Nannoplankton productivity fluctuations and rhythmically bedded pelagic carbonates of the Greenhorn Limestone (Upper Cretaceous). *Paleogeography, Palaeoclimatology, Palaeoecology*, 74, 75–86.

Zaborski, P.M., Ugodulunwa, F., Idornigie, A., Nnabo, P. & Ibe, K. (1997) Stratigraphy and structure of the Cretaceous Gongola basin NE. Nigeria. *Bulletin Des Centres de Recherches Exploration-Production*, 21, 153–185.

Zaborski, P.M. (2000) The Cretaceous and Paleocene transgressions in Nigeria and Niger. *Journal of Mining and Geology*, 36, 153–173.

SUPPORTING INFORMATION

Additional supporting information can be found online in the Supporting Information section at the end of this article.

How to cite this article: Usman, M.B., Jolley, D.W., Brasier, A.T. & Boyce, A.J. (2023) Sequence stratigraphical and palaeoenvironmental implications of Cenomanian–Santonian dinocyst assemblages from the Trans-Sahara epicontinental seaway: a multivariate statistical approach. *The Depositional Record*, 00, 1–33. Available from: https://doi.org/10.1002/dep2.260

APPENDIX 1

TABLE A1 Table of palaeoenvironmental synthesis of Yolde Lamja formations. A = absence, L = low M = moderate, H = high, R = rare, env. = environment, IS = inner shelf, Ms = middle shelf, OS = outer shelf, Group 1B-freshwater, Group 2B-oxygenated neritic, Group 3B-cosmopolitan, Group 4B-peridinioid stratified, Group 5B-peridinioid restricted, Group 1A-inner neritic, Group 2A-middle to outer neritic, Group 3A-cosmopolitan, Group 4A-peridinioids stratified, Group 5A-peridinioids restricted.

Stratigraphic unit	**Yolde Formation**	**Dukul Formation**		**Jessu Formation**
Sample	**BBR3-DKY4**	**DKD1-DKD4**	**DKD5-DKD9**	**JN4-S10**
DIVERSITY	L = stress env.	H = less stress env.	M = less stress env.	M = less stress env.
DOMINANCE	H = stress env.	H = stress env.	H = stress env.	M = less stress env.
P/G	A	L = L. productivity	M = H. productivity	M = M. productivity
DCA				
Group 1A	A	A	A	H = outer shelf open circulation
Group 2A	R	M = MS to OS open circulation	L = restricted circulation	H=IS to OS open circulation
Group 3A	R	A	H = restricted circulation	H = restricted circulation
Group 4A	R	M = restricted circulation	H = restricted circulation	H = restricted circulation
Group 5A	R	L = open circulation	M = restricted circulation	L = open circulation
Synthesis	littoral, high mixing	shallow, mixed water mass	shallow, restricted water	OS, mixed water mass

Stratigraphic unit	**Sekule Formation**		**Sekule-Numanha Formation**	**Numanha Formation**
Sample	**GWS3-GW6**	**YOLS30-GUN11**	**GUN12-AY5**	**AYS3-AYS12**
DIVERSI-TY	M = less stress env.	M = less stress env.	H = less stress env.	L = stress env.
DOMINA-NCE	L = less stress env.	H = stress env.	L = less stress env.	H = stress env.
P/G	M = M. productivity	L = L. productivity	M = M. productivity	L = L. productivity
DCA				
Group 1B	L = low plume	M = moderate plume	v.L = low plume	L = low plume
Group 2B	H = OS, open circulation	H = OS, open circulation	H=OS, open circulation	M = MS to OS, open circulation
Group 3B	L = open circulation	L = open circulation	H = restricted circulation	A
Group 4B	M = restricted marine	L = open circulation	H = restricted circulation	A
Group 5B	M = restricted marine	L = open circulation	A	A
Synthesis	MS, restricted water	mid-outer shelf, mixed water	OS, stratified water	outer shelf, mixed water

S11-S14	LAJ9-BEJ3A	BEJ7-BEJ5	BEJ4-CHY17	CHY18-CH4
H = less stress env.	M = less stress env.	L = stress env.	M = less stress env.	M = less stress env.
L = less stress env.	M = less stress env.	H = stress env.	H = stress env.	M = less stress env.
H=H. productivity	L = Low productivity	M = M. productivity	M = M. productivity	H=H. productivity
A	M = OS open circulation	H=OS open circulation	A = shallow shelf	L = restricted marine
L = restricted circulation	M = IS to OS open circulation	H=IS to OS open circulation	H = open circulation	L = restricted circulation
H = restricted circulation	M = low mixing	L = open circulation	M = low mixing	L = low mixing
M = restricted circulation	M = restricted circulation	L = open circulation	L = open circulation	M = restricted circulation
H = restricted circulation	M = restricted circulation	A = open circulation	L = open circulatione	M = restricted circulation
OS, restricted circulation	OS restricted stratified water	OS, open marine	MS to OS, mixed water	OS, restricted water

		Lamja Formation		
AYS14-AYS23	AYS25	AZN4-LAL5	LAL6	LAL-LAL16
H = less stress env.	H = less stress env.	M = less stress env.	H = less stress env.	L = stress env.
L = less stress env.	L = less stress env.	H = stress env.	L = less stress env.	H = stress env.
H=H. productivity	M = M. productivity	L = low productivity	H=H. productivity	L = L. productivity
A = low plume	L = low plume	L = low plume	A = low plume	H = high plume
H=OS, open circulation	H=OS, open circulation	M = MS to OS open circulation	H=OS, open circulation	L = littoral
M = restricted marine	H = restricted circulation	M = restricted circulation	H = restricted circulation	v. L = open circulation
M = restricted marine	H = restricted circulation	M = restricted circulation	H = restricted circulation	A = open circulation
A	L = restricted circulation	A	M = restricted circulation	A = open circulation
OS, stratified water	OS, stratified water	OS, mixed water	IS to OS, stratified water	littoral, high basin mixing